FINAL Copy
1 9/25/98

Ventifacts at the Pathfinder landing site

N. T. Bridges,[1] R. Greeley,[2] A. F. C. Haldemann,[1] K. E. Herkenhoff,[1,4] M. Kraft,[2] T. J. Parker,[1] and A. W. Ward[3]

Submitted to

Journal of Geophysical Research

March 1998

last Revised

7 July 1998

Abstract. About half of the rocks at the **Mars Pathfinder Ares Vallis** landing site appear to be **ventifacts**, rocks abraded by windborne particles. Comparable resolution images taken by the **Imager for Mars Pathfinder (IMP)** camera and the Viking landers show that ventifacts are more abundant at the Pathfinder site. The ventifacts occur in several forms, including rocks with faceted edges, finger-like projections, elongated pits, flutes, grooves, and possible rills. The trends of elongated pits, flutes, grooves, and rills cluster at ~280-330° clockwise from north and generally dip 10-30° away from their trend direction. These orientations are indicative of southeast to northwest winds and differ from the trend of wind tails at the landing site, the direction of local wind streaks, and predictions of the **Global Circulation Model**, all of which indicate northeast to southwest winds. The disparity between these data sets strongly suggests that local circulation patterns have changed since the abrasion of the ventifacted rocks. The greater number of ventifacts at the Pathfinder site compared to either of the Viking sites is most easily explained as being due to a larger supply of abrading particles, composed of either sand-sized grains or indurated dust aggregates, and higher surface roughness, which should increase the momentum of saltating grains. The Pathfinder ventifacts may have formed shortly after the deposition of outflow channel sediments nearly 2 Gry ago, when a large local supply of abrading particles should have been abundant and atmospheric conditions may have been more conducive to rock abrasion from saltating grains. Based on how ventifacts form on Earth, the several ventifact forms seen at the Pathfinder site and their presence on some rocks but not on others are probably due to local airflow conditions, original rock shape, exposure duration, rock movement, and to a lesser extent, rock lithology. The abundance of ventifacts at the Pathfinder site, together with other evidence of weathering, indicates that unaltered rock surfaces are rare on Mars.

1. Introduction

Ventifacts are rocks that have been sculpted by windborne particles. The link between their morphology and formation mechanism has been well documented in both field and laboratory studies [*Blake*, 1855; *Kuenen*, 1928; *Schoewe*, 1932; *Sharp*, 1949, 1964, 1980; *Whitney and Dietrich*, 1973; *Dietrich*, 1977a,b; *Whitney*, 1978]. Terrestrial ventifacts are located in areas where high-velocity, generally unidirectional winds occur or prevailed in the past. A supply of projectiles capable of eroding rocks is also required, although too great a quantity can decrease abrasion through clumping of silt-sized grains and kinetic interactions between rebounding and incoming particles [*Wood and Espenschade*, 1965; *Suzuki and Takahashi*, 1981; *Greeley and Iversen*, 1985]. Ventifacts generally form in areas lacking vegetation or other obstacles that can act as wind shields. All of these requirements restrict ventifact formation to arid regimes. They form from all types of rocks but are favored on heterogeneous rocks, which become preferentially pitted due to etching of soft components [*Mutch et al.*, 1977]. The morphology and orientation of ventifacts and their component features are a function of the direction of the wind that carried the abrading particles. As such, ventifacts serve as modern and paleo wind indicators and offer insight into ancient climatic regimes.

Three broad categories of ventifacts are recognized in natural terrestrial settings [*Greeley and Iversen*, 1985]: (1) Rocks with wind cut faces or facets, (2) rocks with polished or etched surfaces, and (3) rocks marked by indentations. The last category includes pits, flutes, grooves, and rills. Pits are indentations with rounded to sub-rounded edges, commonly located on rock faces inclined 55-90° to the prevailing wind direction. Most pits form by wind enlarging preexisting inhomogeneities in the rock, such as cracks, soft minerals,

vesicles, or chemically etched regions [*Mutch et al.*, 1977; *McCauley et al.*, 1979; *Greeley and Iversen*, 1985]. Pits are commonly elongated parallel to the prevailing wind direction and as such are transitional with flutes. Flutes are U-shaped in cross section and can be up to 15 cm long [*Sharp*, 1949]. They are found on rock edges oriented ~40° to the wind and commonly merge with more groove-like forms on the upper rock surface. Grooves are located on the top surfaces of rocks, have U-shaped cross sections, and have lengths up to half a meter [*Greeley and Iversen*, 1985]. Rills are subtle linear structures with widths less than 6 mm. Their orientation is not dependent upon the prevailing wind direction, suggesting that other processes, such as chemical weathering, may also play a role in their formation [*Whitney and Dietrich*, 1973; *Greeley and Iversen*, 1985].

Mars has been modified by aeolian processes more than any other solid planet in the solar system. Although weathering induced by wind occurs on Venus and Earth [*Greeley and Iversen*, 1985; *Greeley et al.*, 1992], the surfaces of these planets are by and large much younger than Mars' surface and have been extensively modified by recent volcanism, tectonism, and, in the case of Earth, water. The well preserved wind features on Mars provide a map of present weather conditions and a record of past climatic regimes. The major effects of wind on the geology of the Martian surface are the removal and deposition of dust and sand, the sculpting of landforms into yardangs, and the erosion of rocks by airborne particles to form ventifacts. Because ventifacts are carved from solid rock, they are one of the best preserved wind-produced features on the planet. Martian conditions are favorable for the creation of these forms. On Mars, the velocity of saltating sand grains is expected to be higher than on Earth, causing longer and flatter trajectories that should enhance rock gouging and ventifact formation [*White*, 1979; *Greeley et al.*, 1982]. Some possible ventifacts in the form of faceted rocks, flutes, and circular to elongated pits were suggested in Viking lander images [*Binder et al.*, 1977; *Mutch et al.*, 1977; *Viking Lander Team*, 1978; *McCauley et al.*, 1979]. Many Viking rocks are also perched on pedestals of soil, suggesting aeolian scour on the rocks' undersides, as has been observed in terrestrial deserts [*McCauley et al.*, 1979]. The ventifact-like forms and scouring at the Viking Landing sites imply that aeolian abrasion has modified these surfaces.

The Pathfinder landing site provides a third surface data set for studying aeolian processes and products on Mars. It is rich in aeolian features and, as will be shown, has abundant ventifacts that exceed in number those observed at the Viking sites. An overview of all aeolian aspects of the Pathfinder landing site is provided in a companion paper [*Greeley et al.*, this issue]. The intent of this paper is to first document the morphology, morphometry, position, and orientation of ventifact features as seen by the Sojourner's forward cameras and the lander's Imager for Mars Pathfinder (IMP). Interpretation and discussion of the results, as they pertain to local and Martian geology and the planning of future missions, follow. We show that the landing site has a wide variety of ventifact forms indicative of significant aeolian abrasion over the last 2 Gyr and argue that most of this activity was induced

by winds with a modal direction different from that of today. Although the data support several possibilities, a model whereby the flutes formed by aeolian abrasion from an ancient ephemeral supply of sand deposited by the Ares/Tiu floods is most consistent with our observations. We conclude that unaltered rock surfaces are rare at the Pathfinder site and probably over much of the Martian surface.

2. Ventifact Morphology at the Pathfinder Landing Site

About half of the rocks observed at the Pathfinder landing site exhibit characteristics strongly indicative of aeolian abrasion. With the plethora of rocks observed by the IMP camera [*Mars Pathfinder*, 1997, Plate 5, p. 1734], many of which can be finely resolved using super resolution techniques [*Kanefsky et al.*, 1998; *Parker*, 1998], a complete survey of all ventifact forms has yet to be completed. Nevertheless, an examination of rocks observed in many IMP and in all 384 rover images reveals a diversity of morphologies very similar to that found on terrestrial ventifacts.

Figure 1 compares putative ventifacts at the Pathfinder site with terrestrial analogs. Figure 1a shows a faceted gneiss at Garnet Hill, California compared to the Mars rocks Wedge (left) and Stump (right). Both the gneiss and Wedge are comparable in size, as shown by the scale markers (10 cm at the distance of the front edge of the rocks). Both have flat faces that meet at sharp edges. The smaller rock Stump also appears to have facets oriented in a similar direction to those on Wedge. Another rock, Squash, has finger-like, faceted projections analogous to ventifacted conglomerates and other heterogeneous rocks on Earth, whose clasts are more resistant to abrasion than the softer matrix (e.g., chert blebs in limestone found at Garnet Hill). It is possible that these and other faceted rocks at the Pathfinder site owe their shapes to processes other than wind, as there are a number of physical mechanisms that can produce angular shapes. Apart from Wedge, Stump and portions of Squash, faceted rocks analogous to terrestrial ventifacts are relatively scarce at the Pathfinder site.

The most convincing ventifacts at the Pathfinder site are indentations in the form of pits, flutes, grooves, and possible rills. The Mars rock Stimpy is pocked by subcentimeter sized pits on its side that transition to flutes toward the top. The rock is analogous to terrestrial basalts, such as the one at Amboy Lava Field, California that has had many of its vesicles abraded into flutes (Figure 1b). Although pits on many Martian rocks could be vesicles [*Binder et al.*, 1977; *Mutch et al.*, 1977], chemically etched cavities [*Allen and Conca*, 1991], or sockets of disaggregated conglomerates [*Rover Team*, 1997b], the transition of pits to fluted forms on Stimpy and other rocks implies that many pits are aeolian in origin. Such transitions are common on many terrestrial ventifacts [*Greeley and Iversen*, 1985]. Flutes are even more apparent on the rock Moe, bearing a strong resemblance to fluted rocks on Earth, such as the Garnet Hill diorite shown in Figure 1c. Many of the flutes in both rocks overlap, and in the case of Moe, small flutes are located within larger flutes. Grooves at

the Pathfinder site are not as apparent as pits and flutes, probably because few upper rock surfaces, where grooves are expected, can be clearly seen by the IMP and rover cameras. The Mars rocks Flat Top, Little Flat Top, and Flute Top have planar upper surfaces that exhibit groove-like morphologies. The grooves look similar to grooves found on terrestrial ventifacts, such as a gneiss at Garnet Hill (Figure 1d). Grooves in the surface of Flat Top are clearly seen in close-up images from the rover. Rills are difficult to identify because they are small (< 6 mm wide) and subtle. The pervasive linear texture on the Mars rock Half Dome is analogous to rills seen on terrestrial ventifacts, such as those in the Garnet Hill gneiss shown in Figure 1e. The non-fluted linear texture on Half Dome and that on some other rocks at the landing site could, however, also be primary and not aeolian in nature [*McSween et al.*, this issue]. Some strongly forward-scattering rock surfaces are observed at the Pathfinder landing site [*Johnson et al.*, this issue]. Their photometric properties are consistent with terrestrial rock varnish coatings but may also be the result of surfaces polished by aeolian abrasion. Elongated pits, flutes, and grooves at the Pathfinder landing site are most consistent with formation by aeolian abrasion. Faceted rocks or faceted portions of rocks, circular pits, rills, and forward scattering rock surfaces are likewise consistent with ventifaction but could also form by other mechanisms.

3. Comparison Between Ventifacts at the Pathfinder Landing Site and the Viking Landing Sites

To determine if ventifacts are more common at the Pathfinder landing site than at the Viking sites, IMP images were compared to Viking lander frames. This approach avoided the bias inherent in using close-up rover images, which are not available for the Viking sites. The IMP resolution of 1 mrad/pixel is below Viking's 0.7 mrad/pixel [*Smith et al.*, 1997b]. To produce comparable resolution images, multiple IMP frames of the same scene were co-added to produce "super resolution" pictures [*Parker*, 1998] and then degraded to a resolution of ~ 0.7 mrad/pixel. Figure 2 shows an IMP mosaic of the southwestern part of the landing site (azimuth range of 190° to 275°) scaled to Viking resolution. Despite representing less than a quarter of the whole landing site panorama, many ventifacts are apparent. Flutes are visible on six rocks: Geordi (at least 3 flutes), Half Dome (≥ 8), Garrak (≥ 3), Mohawk (≥ 2), Grommit (≥ 9), and an unnamed rock (≥ 4). Grooves are apparent on Flat Top and Flute Top, and possible faceted faces are seen on Wedge and Stump. Other ventifact forms may be present, but to be conservative, are not identified. The multiple flutes and grooves visible in the IMP mosaic contrasts with the rock textures at the Viking sites. Although some elongated pits are visible at the Viking sites, even the best examples are not developed into long flutes like those at the Pathfinder site (Figure 3) [*Binder et al.*, 1977; *Viking Lander Team*, 1978; *McCauley et al.*, 1979]. These observations strongly suggest that ventifacts are more abundant at the Pathfinder landing site than at the two Viking sites.

4. Ventifact Flute Orientations and Other Attributes

Ventifact indentations on Earth have characteristic sizes, shapes, and locations on rock surfaces. They generally trend parallel or subparallel to the winds that formed them. To further verify that the putative Martian ventifacts were indeed formed by wind and to deduce the direction of these winds, images from the Sojourner rover's front stereo cameras were used to determine the orientation, position, and dimensions of ventifact indentations (hereafter simply referred to as "flutes," except in cases where true flutes are distinguished from elongated pits, grooves, and rills). IMP images were generally not used for this exercise because resolution was mostly inferior to the close-up rover images. About 30-70% of the flutes that were seen in rover images could not be measured because the stereo software was unable to match analogous points in left and right stereo images, preventing determination of position. Details of determining the flute orientations and associated errors are discussed in the appendix.

The orientations of 52 flutes on 15 rocks were recorded (Figure 4 and Plate 1, Table 1). Here and in the subsequent discussion, trends are given in degrees clockwise (E) of north and plunges are oriented downward away from the trend direction (e.g., a flute trending 270° plunges due east). Most of the rocks had 5 or fewer flutes that could be measured. The rock Moe was the most fluted rock seen at the landing site with 20 measurable flutes. Plotting trend and plunge on a polar projection illustrates the distribution of overall flute orientations (Plate 1a) and the mean vector flute orientation for each rock (Plate 1b). The symbol and color of the points on the polar projections correspond to the host rock. Also shown are the minimum (179°), maximum (251°), and average (217°) wind tail azimuths found at the site, the mean trend of wind streaks observed from orbital images (213°), and the direction of maximum wind speed (surface stresses) predicted by the general circulation model (198°) [*Pollack et al.*, 1981; *Greeley et al.*, 1997; *Smith et al.*, 1997a]. For the 165 wind tail measurements made, a modal azimuth of 216° and a standard deviation of 17.63° were found. Twenty-nine wind streaks were measured, also with a modal azimuth of 216° and a standard deviation of 5.36°. The number of eastward-plunging flutes as a function of trend is shown in Plate 1c.

The population of measured flutes as a function of length is shown in Plate 2a. To avoid biasing the statistics by including small rocks that, by their very nature, can only have short ventifact features, only flutes from rocks that are larger than 15 cm are shown. The number of measured flutes is clearly inversely proportional to their length. The longest flutes (actually rills), up to 12.4 cm long, are found on Half Dome. Because most rocks are much larger than the width of flutes, a larger data set can be used to analyze width (Plate 2b). The modal bin for flute width is 0-0.5 cm. As is the case with length, the number of flutes shows an overall decrease with increasing width, although there is some variability between one width bin and the next. The modal flute aspect ratio (length ÷ width) bin is 0 to 2, with the number of flutes decreasing fairly systematically with increasing aspect ratio

(Plate 2c). Flute length is plotted against flute width in Plate 3. The diagonal lines on the plot represent contours of constant aspect ratio (solid) and area (dotted; area is that of an ellipse). As can be seen, the points are fairly scattered, indicating that there is little correspondence between length, width, shape (aspect ratio), and size (area).

The height of measured flutes above the ground varies from less than 2 cm to nearly 30 cm. However, because rocks vary in height, reliable statistics cannot be easily applied to all flute heights as a group. Comparing two independent variables, flute height and length, for individual rocks yields more rigorous statistics (Plate 4). As can be seen in the plot, long flutes are generally higher than short flutes for a given rock.

The length of flutes on rocks wider than 15 cm is compared to plunge and trend in Plate 5. The longest flutes plunge at angles between about 15° and 25° (Plate 5a). Short flutes plunge at all angles. Flute length exhibits a moderate peak between azimuths of about 250° and 320°, with short flutes distributed over a range more than twice as great (Plate 5b).

5. Interpretation

These observations and analyses support the interpretation that ventifacts exist at the Pathfinder landing site and that significant aeolian abrasion has occurred sometime in the past. Most of the putative ventifacts and their component features are very similar to wind-abraded rocks on Earth (Figure 1). The distribution of flute orientations (Plate 1) exhibits two characteristics indicating that the flutes formed by aeolian abrasion: (1) There is a general clustering between azimuths of ~260-330°, indicative of a directionally controlled process and, (2) points cluster radially at plunges of ~10-30°, consistent with terrestrial field and laboratory evidence that most pitting and chopping of rock surfaces occurs at angles inclined ~40-90° to the wind [*Whitney*, 1979; *Sharp*, 1980; *Greeley et al.*, 1982; *Greeley and Iversen*, 1985]. The circular normal distribution of the flutes (Plate 1c) exhibit pronounced peaks between azimuths of 280° and 330°, indicative of winds blowing from southeast to northwest. The trend of groove-like features seen in IMP images on the surface of Flat Top (orange arrows in Plates 1a and 1b; also see Figures 1d and 2) are between 240° and 260°, slightly different than the predominant trend indicated by the flutes but also more easterly than the directions implied by wind streaks, wind tails, and the maximum wind speed predicted by the Global Circulation Model (GCM).

There is some scatter in the data, but this is expected due to natural variations in wind patterns. Some scatter also results from the limited rover image coverage and the limited number of flutes whose orientation could be determined. Sojourner viewed fluted rocks over an azimuth range of ~230°. During the entire mission, very few westward facing rock faces were imaged by the rover. This limits the analysis of flute trends mostly to rock faces dipping toward the southeast, east, and northeast (i.e., when the rover was facing northwest, west, and southwest, respectively). Over this ~180° azimuth range, trends ranging from N-S to E-W can be determined, indicating

that the relatively few flutes with ~N-S trends as opposed to ~E-W is probably not an artifact of sampling. Because flutes are generally carved into the upwind sides of rocks [*Greeley and Iversen*, 1985], the lack of observations of westward facing rock faces cannot rule out winds blowing from the west to the east. The available data set can only discriminate between northerly/southerly and easterly winds, not between northerly/southerly and westerly winds.

The clustered trends of wind tails, wind streaks, and the GCM indicate winds blowing from the northeast to the southwest as opposed to the southeast to northwest direction predicted by the flutes (Plate 1). The differences between these trends is statistically significant. Out of the 52 flutes measured on eastward dipping rock faces, only 10 (19%) have trends that are within the broad 72° range (179-251°) defined by the wind streaks. This is less than half the 21 flutes (72°/180° = 40%) expected if all trends were evenly distributed about the 180° potential azimuth range. Only two out of the 15 measured rocks, "unnamed 2" and "unnamed 7," have mean vectors that plot within this range. In contrast, there are 32 flutes (62%) within the NW wedge defined by 270° to 330°, nearly twice the number expected for an even distribution ([60/180] x 52 = 17). This indicates that the flute trend distribution is not random and is statistically distinct from the wind tail, wind streak, and GCM trends. The rocks Flat Top, Wedge, "unnamed 4," and "unnamed 6" have measurement errors of more than 15° (Table 1). However, they account for only seven measurements, and eliminating them from the statistics does not significantly affect the results.

Treating each flute equally somewhat biases the statistics in favor of rocks with many measured flutes, such as Moe, over those with fewer measured flutes, such as Half Dome. The number of flutes measured on each rock is not necessarily correlated to the number of flutes actually present due to incomplete image coverage and the inability to determine all flute orientations using the stereo software. To avoid this bias, the mean vector of the trends and plunges for all flutes on a given rock were also computed and plotted (Table 1 and Plate 1b). Ten out of the 15 rocks plot in the northwest quadrant, consistent with SE to NW winds and the statistical analyses above.

The length and width of the Martian flutes (Plates 2 and 3) are similar to those of terrestrial ventifact features [*Sharp*, 1949; *Greeley and Iversen*, 1985], although these dimensions by themselves are not strongly diagnostic. More convincing are the relations between flute characteristics and position and orientation on the rock surface (Plates 4 and 5 and Figure 5). Rock abrasion susceptibility varies as a function of position on the rock surface and the angle of that surface to the prevailing wind [*Greeley et al.*, 1982; *Greeley and Iversen*, 1985]. Because the velocities of saltating particles are not a strict function of height, but rather increase along the saltation path length, the variation of particle flux and momentum as a function of height in a natural setting are far more uncertain than impact angle (angle between incoming particle trajectory and rock surface), which is strongly dependent upon the orientation of the rock face. At impact angles greater than about 30° to horizontal, abrasion is inefficient due to the effect

of rebounding particles impeding the momentum of incoming grains [*Greeley et al.*, 1982]. At higher angles, such as those that occur on the upper surfaces of rocks in a saltating layer, particles are able to effectively chip and gouge long grooves into the rock surface (Figure 5). So, the general correlation between flute height and length on a given rock is good evidence that the putative flutes formed by aeolian abrasion (Plate 4). Similarly convincing is the relation between flute length and plunge (Plate 5a). The longest flutes plunge between about 15° and 25°, angles at which maximum abrasion is expected (Figure 5) [*Whitney*, 1979; *Sharp*, 1980; *Greeley et al.*, 1982; *Greeley and Iversen*, 1985]. Finally, the longest flutes have trends that are within the population of most clustered flute trends and indicate that the strongest winds blew from southeast to northwest (Plate 5b). In other words, azimuths that contain the most flutes also have the longest flutes. This is consistent with generally unidirectional, southeast to northwest winds that most effectively abrade rocks along trends parallel to the prevailing wind direction.

6. Discussion

Ventifacts form over time under specific sets of conditions and therefore provide clues to the types, nature, and rates of processes that have operated at the Ares Vallis landing site. The results and interpretations reported here raise several important questions: (1) Why have rocks at the Pathfinder landing site apparently undergone more aeolian abrasion than those at the Viking sites? (2) Why do rocks at the Pathfinder site exhibit different degrees and characteristics of ventifaction, and what accounts for these differences? (3) Why is the wind direction recorded by the flute orientations different than that determined by other means? The answers to these questions are interrelated and offer important insights into aeolian weathering processes on Mars.

6.1. Differences Between the Pathfinder Site and the Viking Sites

Both the Viking and Pathfinder landing sites show evidence of aeolian activity. Both sites are covered with dust, contain drifts, and exhibit some evidence for deflation and abrasion [*Binder et al.*, 1977; *Sagan et al.*, 1977; *Viking Lander Team*, 1978; *McCauley et al.*, 1979; *Smith et al.*, 1997a; *Greeley et al.*, this issue]. Ventifacts, however, appear to be far more unambiguous and abundant at the Pathfinder landing site than at either of the Viking locations (Figures 1-3). Possible physical mechanisms that may account for the disparity between the landing sites are differences in climatic conditions, rock abrasion susceptibility, local airflow conditions, and the supply and characteristics of abrading particles.

Atmospheric conditions, which affect the ability of particles to be picked up by the wind, to saltate, and to erode rocks, are more or less the same at the Pathfinder and Viking 1 landing sites [*Schofield et al.*, 1997]. Wind speeds recorded by Viking 2 were less in a given season than those at Viking 1 and Pathfinder [*Hess et al.*, 1977], yet more putative ventifacts were seen at this site than at Viking 1 [*McCauley et al.*, 1979].

Furthermore, wind speeds measured during the Pathfinder mission were insufficient to cause saltation and particle abrasion (R. Sullivan, personal communication, 1998). Therefore current climatic conditions cannot easily explain the differences in ventifacts between the Pathfinder and Viking sites. Differences in past climatic conditions are a possibility, although it seems that ancient conditions would be very similar at the Pathfinder and nearby Viking 1 sites.

The second possibility, that rocks at the Pathfinder landing site are more susceptible to abrasion than those seen by the Vikings, seems unlikely because ventifacts on Earth are found on all major rock types [*Greeley and Iversen*, 1985]. Furthermore, like rocks at the Pathfinder landing site, most Viking rocks are pitted [*Binder et al.*, 1977; *Viking Lander Team*, 1978; *McCauley et al.*, 1979]. Although some of the pits in the Viking rocks are elongated, none are developed into long flutes like those seen by Pathfinder (Figure 3). Pits on terrestrial rocks are very susceptible to aeolian abrasion and commonly evolve into flutes [*Greeley and Iversen*, 1985]. Pitted rocks at the Viking sites should be susceptible to abrasion like pitted rocks at the Pathfinder site. This is especially true for Viking 1, which has similar weather patterns to those at Pathfinder [*Schofield et al.*, 1997]. However, most of the rocks at the Viking sites have apparently not evolved into ventifacts.

Airflow conditions are dependent upon the regional topography and rock size, shape, and distribution. As such, these conditions differ at all three Mars landing sites. The Pathfinder site is more rugged than the Viking sites [*Smith et al.*, 1997a] and contains more tall rocks. Saltating grains that bounce off hard roughness elements, such as large rocks, will be more apt to recoil to higher elevations than grains that interact with small-scale surfaces [*Greeley and Iversen*, 1985]. These grains should then be entrained in stronger winds and remain aloft for a greater length of time, thereby increasing their momentum and ability to abrade rock surfaces. The rugged nature and abundance of large rocks at the Pathfinder landing site may therefore partially explain the plethora of ventifact and other aeolian abrasion features.

The fourth possibility is that differences in the supply or characteristics of abrading particles account for the landing site disparities. If this is the case, then the ventifact contrasts could be either the result of differences between abrading particle supplies or the makeup of abrading particles. There is evidence for local, albeit small, supplies of abrading particles at the Pathfinder site. Classic barchan duneforms observed by Sojourner are not found at either of the Viking sites [*Greeley et al.*, this issue]. The morphology of these deposits is consistent with a physical makeup of either sand-sized particles or indurated dust aggregates (also known as parna) [*Greeley and Williams*, 1994; *Greeley et al.*, this issue]. The latter possibility is worthy of further consideration. *Greeley et al.* [1982] estimated the susceptibility to abrasion of several target materials impacted by different solid particles under conditions that were believed to match those at the Viking landing sites. The predicted rates were judged as too extreme because they implied that craters and other large-scale features would be erased on a geologic timescale. Greeley et al.

considered the most likely explanation that reconciled theory and observation was that the primary agents for erosion were either of limited supply or were relatively inefficient in causing erosion, such as would be the case if the impacting particles were aggregates instead of solid grains. Although both solid grains and indurated dust aggregates satisfy the requirement for local repositories of abrading particles at the Pathfinder site, parna also fulfills the need for the grains to be inefficient enough at abrading so that rocks are not completely worn away. Nonaggregated dust has also been advocated as a rock abrading agent on Mars [*McCauley et al.*, 1979]. Over the long timescales of erosion that have occurred at the Pathfinder site, dust erosion cannot be ruled out. However, it is puzzling why nonaggregated dust, which is fairly ubiquitous on Mars, should more effectively erode rocks at the Pathfinder site than rocks at the Viking sites. Therefore sand-size grains or indurated dust-aggregates seem more likely.

A likely source of sand-size grains was sediments deposited at the mouths of the Ares/Tiu channels. This hypothesis explains why a potential supply of abrading particles was available to the Pathfinder site, where ventifacts are abundant, but not to areas located farther from the channels, such as the Viking Lander 1 site, where ventifacts are scarce. This is consistent with field studies on Earth that show a correlation between sediment supply and the rate of aeolian transport [*Williams and Lee*, 1995]. Because wind directions in ancient climatic regimes were probably different than winds of today and because any sand supply should be reduced or become exhausted over time, this hypothesis is consistent with the discrepancy in wind directions derived from flutes versus those from wind tails, wind streaks, and the general circulation model.

6.2. Differences Among Rocks at the Pathfinder Site

About half of the rocks viewed in close-up IMP and rover images appear to have a variety of ventifact features, whereas other rocks seem to be relatively unaffected by wind abrasion. Insight into the causes of these differences can be gleaned from what is known about the formation of ventifacts in natural settings on Earth. The characteristics of terrestrial ventifact features in a local area are highly variable, even among rocks of the same lithology. These differences are due in part to (1) original rock shape and texture, (2) local atmospheric flow patterns, (3) rock exposure duration, and (4) rock movement during the abrasion period [*Greeley and Iversen*, 1985].

The original shape of rocks is highly variable and independent of composition. Rocks shapes at the Pathfinder site vary from rounded to angular, with the former probably deposited by the Ares/Tiu Valles floods and the latter as impact ejecta [*Smith et al.*, 1997a]. Rock texture is also variable and can be independent of composition. However, because pits and other heterogeneities in rocks are commonly exploited by local windflow and modified into flutes [*Mutch et al.*, 1977; *McCauley et al.*, 1979; *Greeley and Iversen*, 1985], some rock types, such as vesicular volcanic rocks, are more apt to be heterogeneous than others and evolve into ventifacts.

Local atmospheric flow patterns may be highly variable at the Pathfinder site. Small-scale topography should influence the airflow on rocks and rocks' susceptibility to abrasion by airborne particles. This topography is a function of local crests and troughs and rock size, shape, and distribution. A full analysis of this factor requires detailed mapping of the site integrated with a large catalog of rock characteristics, a task that is beyond the scope of this paper but that is currently under way.

The emplacement ages of the rocks at the Pathfinder site correspond to the major geologic events in the region, the Ares/Tiu floods and deposition of crater ejecta from local impacts. The floods occurred in the late Hesperian to early Amazonian (~ 1.8 Ga) and the cratering events at times thereafter [*Scott and Tanaka*, 1986; *Parker and Rice*, 1997; *Tanaka*, 1997]. Although atmospheric pressures could have been similar to those of today [*Fanale et al.*, 1992], evidence for stable, large bodies of water at this time argue for higher pressures [*Parker et al.*, 1993]. If this was the case, then this early putative thick Martian atmosphere may have been a more effective transporting agent of abrading particles than the thin one of today. Rocks deposited by the floods, in addition to being exposed for a longer time, may have also been subject to more effective abrasion than rocks deposited later by impacts. In addition to these events, aeolian burial and removal of soil have probably affected rock exposure duration. Dunes and drifts visible in IMP and rover images have undoubtedly migrated with time, alternately shielding and exposing rocks to aeolian abrasion. Horizontal boundaries between lower bright and upper dark regions on many rocks at the Pathfinder site are suggestive of a former ~ 5 cm thick soil layer that has subsequently been deflated by the wind [*Greeley et al.*, this issue]. Based on orbital images, exumation on a larger scale also seems to have occurred in Chryse Planitia [*Greeley et al.*, 1977, 1982; *Parker and Rice*, 1997]. If episodes of deflation and deposition have occurred at the Pathfinder site, then portions of and perhaps entire rocks may have been protected from aeolian scour for unknown periods of time. It is even possible that a few rocks could have been exposed elsewhere on the surface prior to being plucked by the floods or ejected by impacts, adding further uncertainty to their exposure duration. It is therefore likely that the rocks at the Pathfinder landing site have been exposed over a range of time periods and that this has had an effect on their abrasion history.

The fourth factor, movement of rocks during the abrasion period, is also possible. As discussed above, rocks could have been exposed at the surface before being transported to their present location by the floods or impact events. If this happened, it may account for some of the variability in flute orientations (Plate 1).

6.3. Flute-Derived Wind Directions Versus Other Estimates

The wind directions inferred by flute orientations are generally southeast to northwest, whereas those predicted by the trend of wind tails and wind streaks and the GCM are approximately northeast to southwest. There are two likely possibilities that explain the discrepancy between the flute

orientations and the other predictions, both of which indicate significant variability in Martian weather patterns over time. One is that the latest storm or storms that produced the wind tails and streaks blew more from the northeast than is typical for this area. Alternatively, the winds responsible for fluting may have occurred over short periods of time during a different climatic regime(s) but were stronger than winds of today and were able to carry particles with sufficient momentum to abrade rock surfaces. Easterly winds in the tropical latitudes, including the Pathfinder landing site, are strongest during the equinoxes (L_s = 0° and 180°) [*Haberle et al.*, 1993]. Periodically during intervals of the modern ~125,000 year obliquity oscillation cycle, the equinoxes occur at perihelion, in which case stronger easterly winds would be expected. In this case, the integrated effect of strong, short-term, easterly winds over time would produce the flutes. A problem with this hypothesis is that there are no obvious large sources of abrading particles that could be harnessed by these putative winds. A more likely possibility is that ancient winds formed the flutes when a plentiful supply of abrading particles was available, such as the outflow channel sediments deposited approximately 1.8 Gyr ago. We prefer this model, although the data cannot rule out other competing hypotheses.

6.4. Implications for Martian Geology and Exploration

The abundance and nature of ventifacts at the Pathfinder landing site have important implications for Martian geology. The evidence provided by the flute orientations that wind directions have shifted through Martian history is consistent with other observations indicating that Mars' climate changes with time. Variations in Mars' orbital elements and precession of its spin axis are believed to affect the exchange of volatiles and dust between the polar caps, as indicated by bands in the polar layered terrain interpreted to be dust-poor and dust-rich layers [*Kieffer and Zent*, 1992; *Thomas et al.*, 1992]. These putative climatic fluctuations have undoubtedly had an effect on local wind directions and intensities. The fact that ancient wind directions are probably recorded by the flutes at the Pathfinder landing site offers the exciting prospect that analyses of ventifacts at future Mars landing sites may provide insight into paleoclimatic conditions.

Viking Lander images indicated only a limited degree of rock abrasion on Mars [*Binder et al.*, 1977; *Mutch et al.*, 1977; *Viking Lander Team*, 1978; *McCauley et al.*, 1979]. The results reported here show evidence for greater abrasion, at least for some regions of the planet. Martian rock surfaces seem to be metastable and erode through time. The amount of rock that has been lost to abrasion over Martian history is difficult to estimate, but is probably not insignificant. The evidence for abrasion, together with observations that indicate significant dust contamination of rock surfaces and perhaps the formation of silica-rich weathering rinds [*Bridges et al.*, 1997; *McSween et al.*, this issue], imply that original rock surfaces are rare on Mars. Whereas dust deposits and weathering rinds will alter the chemistry of rock surfaces, aeolian scour will act to remove them. The interplay between these forces will determine how much rocks are weathered chemically versus

physically. This should be considered when trying to extract chemical and mineralogical information from remote spectral instruments such as IMP. This should also be factored into sample collection strategies on future Mars missions, which have as one of their goals the collection and analyses of unaltered Martian rock. The retrieval of pristine rocks on these missions will probably be difficult, in many cases necessitating the use of drills such as that planned for the Athena rover. Ventifacts, targets that have been "drilled" naturally by the wind, may offer the best samples of pristine Martian rock.

7. Conclusions

1. About half the rocks at the Pathfinder landing site have shapes or features similar to those of terrestrial ventifacts. The types of ventifacts found include rocks with faceted edges, finger-like projections, elongated pits, flutes, grooves, possible rills, and possible polished surfaces.

2. Elongated pits, flutes, grooves, and rills have trends and plunges that cluster at ~280-330° and ~10-30°, respectively. The trends are indicative of formation by southeast to northwest winds. The plunges are consistent with pitting and chopping of rock surfaces by wind-transported particles. The longest flutes plunge between about 15° and 25°, angles at which maximum aeolian abrasion is expected to occur. They are also oriented nearly parallel to the mean flute orientation, indicating that the abrasion was most effective along azimuths near to the prevailing wind direction. The ~SE to NW wind directions implied by the flute orientations are different from those estimated from the ~NE to SW trends of wind streaks and wind tails and those predicted by the General Circulation Model. Any effects by westerly winds cannot be determined because very few eastward facing rock faces were imaged by the rover.

3. The differences in ventifact characteristics among rocks at the Pathfinder landing site are a function of original rock shape and texture, local airflow patterns, rock movement, time of emplacement, and the duration over which a rock is exposed to the atmosphere. Lithology is probably not as important, although it will have some effect on original rock texture.

4. Ventifacts appear to be much more abundant at the Pathfinder landing site than at either of the two Viking sites. One minor factor may be the higher surface roughness and abundance of large rocks at the Pathfinder site, which should increase the momentum of saltating grains. Other possibilities, such as differences in atmospheric circulation, wind speeds, and rock abrasion susceptibility, seem less likely.

5. The most favored model to explain the differences between the landing sites and the discrepancy in flute orientations is that the flutes formed shortly after the deposition of flood sediments, when the climate may have been different and an ephemeral supply of local sand available.

6. Based on these and other Pathfinder results, unaltered rock surfaces are relatively rare at the Pathfinder landing site and probably over much of Mars. This should be considered when trying to extract compositional information from remote

spectral observations and in the planning of sampling strategies for future Mars missions. Because aeolian scour removes the outer surfaces of rocks, which are probably chemically weathered, the most pristine samples on Mars are likely to be ventifacts.

Appendix

A. Measurement Methods

To measure flute orientations, the positions of flute endpoints in the rover coordinate frame were determined. To convert the orientations to the Mars surface fixed frame (identical to the coordinate frame used on Mars maps), rover position had to be determined. Although Sojourner estimated and recorded its own position and orientation during traverses by dead reckoning, these estimates often deviated from the true values. IMP stereo or monoscopic images of Sojourner at the time of rover imaging were available in many cases and were used to compute the true rover position and orientation ("stereo" and "monoscopic" methods in Table 1). If supporting IMP images were unavailable, several methods were used. Dead reckoning data in the rover image headers, dead reckoning data at the end of a traverse, and the IMP-derived true rover position at the beginning and end of a traverse were used to compute rover positions in mid traverse by estimating the drift in dead reckoning as a function of rover moves ("interpolation" method in Table 1). Where features visible in both rover and IMP images were known relative to IMP, the rover position was computed by tying the location of these image features together ("triangulation" method in Table 1). Once the position of the rover was determined using these techniques, positions of flute endpoints in the rover coordinate frame were transformed to the Mars surface fixed frame and converted to trend and plunge.

Flute elevation was determined by measuring the difference between the height of the middle of a flute and the elevation of the base of the host rock in the Mars surface fixed frame. Flute lengths were taken as the linear distance between the flute endpoints, a good approximation because flutes do not appear to appreciably curve along their length. The accuracy of the JPL stereo software was generally insufficient to determine local position differences on the pixel scale and could not be effectively employed to measure most flute widths. Instead, width was computed by measuring the number of pixels subtended across the semi-minor axis of a flute in rover images. By knowing the average distance of the flute from the rover cameras computed from the stereo program and the average resolution of the cameras (0.003153 radians/pixel [*Rover Team*, 1997a]), the width could be estimated. The uncertainty associated with this method is equal to the image resolution (Table 1) except in cases where the plunge of the flute semi-minor axis deviates significantly from the rover camera plane orientation.

A2. Error Analysis

The two main sources of error in the orientation analyses were the determination of flute orientation in rover images and the estimation of rover orientation. Errors measuring flute positions in rover images affect both trend and plunge values, whereas uncertainties in the rover orientation mostly affect trends. In rover images, a line connecting flute endpoints is made of N pixels and has N -1 pixel-pixel boundaries. The number of pixels depends upon both the flute length and the distance between the rover cameras and the flute. The number of orientations over which the pixels can be arrayed over a 180° range is $4(N\text{-}1)$. This gives a potential degree error within the image plane of $\pm\ 180°/(8[N\text{-}1])$. Values for this uncertainty vary from 0.4° to 4.4° (Table 1).

In cases for which IMP stereo images documented rover position, rover orientation uncertainty was assumed to be a function of the pixel size of the rover in the images and was computed using the method described above (except in this case the number of pixels making up the rover length is substituted for the number of pixels making up the flute length). Where only monoscopic images were available, the error was judged to be twice as poor (i.e., $\pm\ 180°/(4[N\text{-}1])$). It was difficult to estimate the error using the interpolation method because the drift was in most cases probably not a linear function of the number of rover moves. Being conservative, the uncertainty was taken as the difference between the IMP-derived and dead reckoning position at the end of the traverse. The uncertainty using the triangulation method is also difficult to estimate but is probably of the order of 10°. Using all these methods, the error associated with rover position varies from 0.1° to 54°. The total uncertainty in flute trends is computed by summing the errors associated with flute position in rover images and those associated with rover orientation. These vary from 1 to 55°, but in most cases are less than 15° (Table 1).

Acknowledgments. Reviews by R.E. Arvidson, R. Eby, and an anonymous reviewer are gratefully acknowledged. We are also indebted to several individuals, without whose time and intellect this project would not have been possible. J.A. Crisp introduced us to the JPL "Showstereo" stereophogrammetry software, pointed out several references, and provided good discussion. T.E. Litwin helped develop Showstereo and guided us in its use. B.K. Cooper kindly took time to measure several rover positions that assisted our analyses of flute orientations. D.A. Alexander produced stereo-ready images for our use. R.M. Haberle and J.T. Schofield provided insight on Martian atmospheric dynamics. J.R. Johnson helped explain photometric observations of rock surfaces. M.I. Whitney graciously sent us several references and extended write-ups on her work.

The research described in this paper was carried out by the Jet Propulsion Laboratory, California Institute of Technology, under a contract with the National Aeronautics and Space Administration.

References herein to any specific commercial product, process, or service by trade name, trademark, manufacturer, or otherwise, does not constitute or imply its endorsement by the United States Government or the Jet Propulsion Laboratory, California Institute of Technology.

References

Allen, C.C., and J.L. Conca, Weathering of basaltic rocks under cold, arid conditions: Antarctica and Mars, *Proc, Lunar Planet. Sci. Conf., 21*, 711-717, 1991.

Binder, A.B., R.E. Arvidson, E.A. Guinness, K.L. Jones, E.C. Morris, T.A. Mutch, D.C. Pieri, and C. Sagan, The geology of the Viking Lander 1 site, *J. Geophys. Res., 82*, 4439-4451, 1977.

Blake, W.P., On the grooving and polishing of hard rocks and minerals by dry sand, *Am. J. Sci., 20*, 178-181, 1855.

Bridges, N.T., R.C. Anderson, J.A. Crisp, T. Economou, and R. Reid, Separating dust and rock APXS measurements based on multispectral data at the Pathfinder landing site (abstract), *Eos Trans. AGU, 78*, Fall Meeting Suppl., F402-403, 1997.

Dietrich, R.V., Impact abrasion of harder by softer materials, *J. Geol., 95*, 242-246, 1977a.

Dietrich, R.V., Wind erosion by snow, *J. Glaciol., 18*, 148-149, 1977b.

Fanale, F.P., S.E. Postawko, J.B. Pollack, M.H. Carr, and R.O. Pepin, Mars: Epochal climate change and volatile history, in *Mars*, edited by H.H. Kieffer, B.M. Jakosky, C.W. Snyder, and M.S. Matthews, pp. 1135-1179, Univ. of Ariz. Press, Tucson, 1992.

Golombek, M.P., et al., Overview of the Mars Pathfinder mission: Launch through landing, surface operations, data sets, and science results, *J. Geophys. Res.*, this issue.

Greeley, R. and J.D. Iversen, *Wind as a Geological Process on Earth, Mars, Venus, and Titan*, 333 pp., Cambridge Univ. Press, New York, 1985.

Greeley, R. and S.H. Williams, Dust deposits on Mars: The "parna" analog, *Icarus, 110*, 165-177, 1994.

Greeley, R., E. Theilig, J.E. Guest, M.H. Carr, H. Masursky, and J.A. Cutts, Geology of Chryse Planitia, *J. Geophys. Res., 82*, 4093-4109, 1977.

Greeley, R., R.N. Leach, S.H. Williams, B.R. White, J.B. Pollack, D.H. Krinsley, and J.R. Marshall, Rate of wind abrasion on Mars, *J. Geophy. Res., 87*, 10,009-10,024, 1982.

Greeley, R., et al., Aeolian features on Venus: Preliminary Magellan results, *J. Geophys. Res., 97*, 13,319-13,345, 1992.

Greeley, R., R. Sullivan, M. Kraft, P. Smith, M. Malin, R. Kuzmin, M.P. Golombek, and K. Herkenhoff, Aeolian geology and the Mars Pathfinder landing site (abstract), *Eos Trans. AGU, 78*, Fall Meeting Suppl., F395, 1997.

Greeley, R., M. Kraft, G. Wilson, N.T. Bridges, K.E. Herkenhoff, R. O. Kuzmin, M.C. Malin, R. Sullivan, and A.W. Ward, Aeolian features and processes at the Mars Pathfinder landing site, *J. Geophys. Res.*, this issue.

Haberle, R.M., J.B. Pollack, J.R. Barnes, R.W. Zurek, C.B. Leovy, J.R. Murphy, H. Lee, and J. Schaeffer, Mars atmospheric dynamics as simulated by the NASA Ames General Circulation Model, 1, The zonal-mean circulation, *J. Geophys. Res., 98*, 3093-3123, 1993.

Hess, S.L., R.M. Henry, C.B. Leovy, J.A. Ryan, and J.E. Tillman, Meteorological results from the surface of Mars: Viking 1 and 2, *J. Geophy. Res., 82*, 4559-4574, 1977.

Johnson, J.R., et al., Preliminary results on photometric properties of materials at the Sagan Memorial Station, Mars, *J. Geophys. Res.*, this issue.

Kanefsky, B., T.J. Parker, and P.C. Cheeseman, Super-resolution results from Pathfinder IMP (abstract), *Lunar Planet. Sci. XXIX*, 1536, 1998.

Kieffer, H.H. and A.P. Zent, Quasi-periodic climate change on Mars; in Kieffer, in *Mars*, edited by H.H. Kieffer, B.M. Jakosky, C.W. Snyder, and M.S. Matthews, pp. 1180-1218, Univ. of Ariz. Press, Tucson, 1992.

Kuenen, P.H., Experiments on the formation of wind-worn pebbles, *Leische Geol. Melellinger, 3*, 17-38, 1928.

Mars Pathfinder, Foldout plates, *Science, 278*, 1735-1742, 1997.

McCauley, J.F., C.S. Breed, F. El-Baz, M.I. Whitney, M.J. Grolier, and A.W. Ward, Pitted and fluted rocks in the Western Desert of Egypt: Viking comparison, *J. Geophys. Res., 84*, 8222-8232, 1979.

McSween, H. Y., et al., Chemical, multispectral, and textural constraints on the composition and origin of rocks at the Mars Pathfinder landing site, *J. Geophys. Res.*, this issue.

Mutch, T.A., R.E. Arvidson, A.B. Binder, E.A. Guinness, and E.C. Morris, The geology of the Viking 2 landing site, *J. Geophys. Res., 82*, 4452-4467, 1977.

Parker, T.J., "Super resolution" of the Mars Pathfinder landing site, using manual techniques (abstract), *Lunar Planet. Sci. XXIX*, 1817, 1998.

Parker, T.J., and J.W. Rice, Sedimentary geomorphology of the Mars Pathfinder landing site, *J. Geophys. Res., 102*, 25,641-25,656, 1997.

Parker, T.J., D.S. Gorsline, R.S. Saunders, D.C. Pieri, and D.M. Schneeberger, Coastal geomorphology of the Martian northern plains, *J. Geophy. Res., 98*, 11,061-11,078, 1993.

Pollack, J.B., C.B. Leovy, P.W. Greiman, and Y. Mintz, A Martian general circulation experiment with large topography, *J. Atmos. Sci., 38*, 3-29, 1981.

Rover Team, The Pathfinder microrover, *J. Geophys. Res., 102*, 3989-4001, 1997a.

Rover Team, Characterization of the Martian surface deposits by the Mars Pathfinder rover, Sojourner, *Science, 278*, 1765-1768, 1997b.

Sagan, C., D. Pieri, P. Fox, R.E. Arvidson, and E.A. Guinness, Particle motion on Mars inferred from the Viking Lander cameras, *J. Geophys. Res., 82*, 4430-4438, 1977.

Schoewe, W.H., Experiments on the formation of wind-faceted pebbles, *Am. J. Sci., 224*, 111-134, 1932.

Schofield, J.T., J.R. Barnes, D. Crisp, R.M. Haberle, S. Larsen, J.A. Magalhães, J.R. Murphy, A. Seiff, and G. Wilson, The Mars Pathfinder atmospheric structure investigation/meteorology (ASI/MET) experiment, *Science, 278*, 1752-1758, 1997.

Scott, D.H., and K.L. Tanaka, Geologic map of the western equatorial region of Mars; in *Chryse Planitia, Atlas of Mars Geol. Ser., U.S. Geol. Surv. Misc. Invest. Ser. Map., I-1802-A*, 1986.

Sharp, R.P., Pleistocene ventifacts east of the Big Horn Mountains, Wyoming, *J. Geol., 57*, 175-195, 1949.

Sharp, R.P., Wind-driven sand in Coachella Valley, California, *Geol. Soc. Am. Bull., 74*, 785-804, 1964.

Sharp, R.P., Wind-driven sand in Coachella Valley, California: Further data, *Geol. Soc. Am. Bull., 91*, 724-730, 1980.

Smith, P.H., et al., Results from the Mars Pathfinder camera, *Science, 278*, 1758-1765, 1997a.

Smith, P.H., et al., The Imager for Mars Pathfinder experiment, *J. Geophys. Res., 102*, 4003-4025, 1997b.

Stoker, C., T. Blackmon, J. Hagan, B. Kanefsky, C. Neveu, K. Schwehr, M. Sims, and E. Zbinden, MarsMap: Analyzing Pathfinder data using virtual reality (abstract), *Eos Trans. AGU, 78*, Fall Meeting Suppl., F403, 1997.

Suzuki, T., and K. Takahashi, An experimental study of wind abrasion, *J. Geol., 89*, 23-36, 1981.

Tanaka, K.L., Sedimentary history and mass flow structures of Chryse and Acidalia Planitiae, Mars, *J. Geophy. Res., 102*, 4131-4149, 1997.

Thomas, P., S. Squyres, K. Herkenhoff, A. Howard, and B. Murray, Polar deposits on Mars, in *Mars*, edited by H.H. Kieffer, B.M. Jakosky, C.W. Snyder, and M.S. Matthews, pp. 767-795, Univ. of Ariz. Press, Tucson, 1992.

Viking Lander Team, *The Martian Landscape, NASA Spec. Publ., SP-425*, 160 pp., 1978.

White, B.R. Soil transport by winds on Mars, *J. Geophys. Res., 84*, 4643-4651, 1979.

Whitney, M.I., The role of vorticity in developing lineation by wind erosion, *Geol. Soc. Am. Bull., 89*, 1-18, 1978.

Whitney, M.I., Electron micrography of mineral surfaces subject to wind-blast erosion, *Geol. Soc. Am. Bull., 90*, 917-934, 1979.

Whitney, M.I., and R.V. Dietrich, Ventifact sculpture by windblown dust, *Geol. Soc. Am. Bull., 84*, 2561-2582, 1973.

Williams, S.H., and J.A. Lee, Aeolian transport rate: An example of the effect of sediment supply, *J. Arid Environ., 30*, 153-160, 1995.

Wood, C.D. and P.W. Espenschade, Mechanisms of dust erosion, *Soc. Automotive Eng., 73*, 515-523, 1965.

Figure Captions

Figure 1. Comparison between terrestrial ventifacts and analogous rocks at the Pathfinder landing site. (a) Faceted rocks. The left frame is a photograph of a gneiss ventifact block at Garnet Hill, California. The pocket knife is 10 cm long. The right frame is an IMP super resolution image of the rocks Wedge (left) and Stump (right, below black bar). Scale bar is 10 cm long at the front top edge of Stump.

Figure 1b. Pitted rocks. The left frame is a vesicular basalt at Amboy Lava Field, California. Note that the vesicles on the upper surfaces of the rocks are more elongated than those on the sides. The right frame shows the Mars rock Stimpy as viewed by the rover's left front camera. Note that the pits on Stimpy increase in elongation with height above the surface. The scale bar corresponds to a length of 10 cm at the back edge of the rock.

Figure 1c. Fluted rocks. The left frame shows a fluted diorite at Garnet Hill. Note that the flutes cut across bands of aligned feldspars (white splotches) in the rock. The right frame is an image of the Mars rock Moe taken by the rover's left front camera. Moe is the most fluted rock seen at the landing site. This image clearly shows small flutes within larger flutes. The scale bar corresponds to a length of 10 cm at the back edge of the rock.

Figure 1d. Grooved rocks. The left frame is a grooved gneiss at Garnet Hill. The ruler on top of the rock is 30 cm (1 foot) long. The middle frame is a super resolution IMP image of the rock Flat Top. The arrows show the orientation of groove-like features on the surface of the rock. The scale bar corresponds to a length of 10 cm near the front of Flat Top. The right frame is a close-up view of the side of Flat Top as seen by Sojourner's left front camera. Note that the grooves on Flat Top are cut into the rock. Elongated pits are also visible on the side of Flat Top below the grooves. Scale bars corresponds to a length of 10 cm near the front surface of the rock.

Figure 1e. Rocks with possible rills. The left frame shows rills, oriented from lower left to upper right, cut into the surface of a gneiss at Garnet Hill. The pocket knife is 10 cm long. The right frame shows the Mars rock Half Dome as viewed by the rover's right camera. Rill-like features are best seen on the upper part of the rock, trending from lower left to upper right. Scale bar corresponds to a length of 10 cm near the upper part of Half Dome.

Figure 2. The Pathfinder landing site viewed by IMP over an azimuth range of 190° (left) to 275° (right). The mosaic is scaled to match the resolution of the Viking lander cameras (0.7 mrad/pixel). Areas containing abundant ventifacts on rocks are indicated by single-sided arrows. The trend of grooves on the rocks Flat Top and Flute Top are indicated by double-sided arrows. Wedge and Stump have faceted edges that may have formed by aeolian abrasion. Hints of additional flutes are apparent on other rocks, but their true nature cannot be discerned at this resolution.

Figure 3. A comparison between raw Pathfinder IMP (left, 1 mrad/pixel) and Viking Lander 2 (right, 0.7 mrad/pixel) rocks with ventifact-like features. The large, foreground rocks in both images are 24 cm across. Even with the coarse resolution of IMP, flutes can be seen on the foreground rock (Grommit). The VL 2 frame (21B021) shows some of the best examples of aeolian abrasion features at either Viking site. Although elongated pits are visible, no flutes such as those seen on Grommit or those visible on rocks in other IMP images (Figures 1 and 2) are apparent.

Figure 4. Schematic map of the Pathfinder landing site showing ventifacted rocks discussed in this paper. North is to the top and coordinate axes are in meters. Rocks shown as black ovals and labeled in bold print were analyzed by Sojourner's alpha proton x-ray spectrometer. Crosses and labels in normal font show the location of other rocks. Dark lines delineate the rover traverse path (also refer to maps by *Golombek et al.* [this issue]).

Plate 1a. Polar projection showing trends and plunges of flutes at the Pathfinder landing site. The circumferential axis represents trend and the radial axis plunge. Plunges are oriented downward toward the center of the plot and increase inward. Colored symbols correspond to the rocks upon which the flutes are located. Colored lines projecting outward from the edge of the plot show the direction the rover cameras were pointed when images used to derive flute orientations were taken (e.g., for the Moe observations, the rover had a heading of 271°). The association between the rock and rover orientation symbols is shown in the legend at right. The orange arrows represent the range of trends of groove-like features on the surface of Flat Top, as determined from IMP images projected to a bird's eye view using the Ames MarsMap virtual reality system [*Stoker et al.*, 1997]. Solid black arrows are minimum, average, and maximum values of local wind tail directions [*Greeley et al.*, 1997; *Smith et al.*, 1997a]. Arrow with large dashes represents the average trend of wind streaks as seen in orbital images [*Greeley et al.*, 1997; *Smith et al.*, 1997a]. Arrow with small dashes is the predominant wind direction predicted by the General Circulation Model [*Pollack et al.*, 1981; *Greeley et al.*, 1997; *Smith et al.*, 1997a].

Plate 1b. Same as Plate 1a, except showing the mean vector of flutes on each rock.

Plate 1c. Circular normal distribution of flute trends for flutes with azimuths of 180°-360°.

Plate 2. The number of flutes compared to flute dimensions and shape. The color or pattern of the bars corresponds to the rock upon which the flutes are located. (a) Number of measured flutes as a function of length.

Plate 2b. Number of measured flutes as a function of width.

Plate 2c. Number of measured flutes as a function of aspect ratio (length ÷ width).

Plate 3. Flute length versus width. The color or type of symbol corresponds to the rock upon which the flutes are located. Solid diagonal lines are aspect ratios, with values shown in bold type where the lines intersect the plot edge. Areas, assuming a flute shape of an ellipse, are shown as dotted diagonal lines, with values in cm^2 in italic type.

Plate 4. Flute height (the elevation of the middle of the flute above the surface) versus length. The color or type of symbol corresponds to the rock upon which the flutes are located. Because large rocks can have flutes over a range of sizes, as opposed to small rocks which can only have small flutes, only flutes on rocks that are larger than 15 cm are shown. The height of the rocks as seen from the IMP camera is indicated by the horizontal bars (note, portions of the rocks not easily seen by IMP can be higher than these values).

Plate 5a. Flute length versus plunge.
Plate 5b. Flute length versus trend. The solid lines are the minimum, average, and maximum values of local wind tail directions, the line with large dashes represents the average trend of wind streaks as seen in orbital images, and the line with small dashes is the predominant wind direction predicted by the General Circulation Model [*Pollack et al.*, 1981; *Greeley et al.*, 1997; *Smith et al.*, 1997a].

Figure 5. Schematic illustration of the effect of impact angle and rock face orientation on the efficiency of abrasion. Plot from *Greeley et al.* [1982].

Figure 1. Comparison between terrestrial ventifacts and analogous rocks at the Pathfinder landing site. (a) Faceted rocks. The left frame is a photograph of a gneiss ventifact block at Garnet Hill, California. The pocket knife is 10 cm long. The right frame is an IMP super resolution image of the rocks Wedge (left) and Stump (right, below black bar). Scale bar is 10 cm long at the front top edge of Stump.
Figure 1b. Pitted rocks. The left frame is a vesicular basalt at Amboy Lava Field, California. Note that the vesicles on the upper surfaces of the rocks are more elongated than those on the sides. The right frame shows the Mars rock Stimpy as viewed by the rover's left front camera. Note that the pits on Stimpy increase in elongation with height above the surface. The scale bar corresponds to a length of 10 cm at the back edge of the rock.
Figure 1c. Fluted rocks. The left frame shows a fluted diorite at Garnet Hill. Note that the flutes cut across bands of aligned feldspars (white splotches) in the rock. The right frame is an image of the Mars rock Moe taken by the rover's left front camera. Moe is the most fluted rock seen at the landing site. This image clearly shows small flutes within larger flutes. The scale bar corresponds to a length of 10 cm at the back edge of the rock.
Figure 1d. Grooved rocks. The left frame is a grooved gneiss at Garnet Hill. The ruler on top of the rock is 30 cm (1 foot) long. The middle frame is a super resolution IMP image of the rock Flat Top. The arrows show the orientation of groove-like features on the surface of the rock. The scale bar corresponds to a length of 10 cm near the front of Flat Top. The right frame is a close-up view of the side of Flat Top as seen by Sojourner's left front camera. Note that the grooves on Flat Top are cut into the rock. Elongated pits are also visible on the side of Flat Top below the grooves. Scale bars corresponds to a length of 10 cm near the front surface of the rock.
Figure 1e. Rocks with possible rills. The left frame shows rills, oriented from lower left to upper right, cut into the surface of a gneiss at Garnet Hill. The pocket knife is 10 cm long. The right frame shows the Mars rock Half Dome as viewed by the rover's right camera. Rill-like features are best seen on the upper part of the rock, trending from lower left to upper right. Scale bar corresponds to a length of 10 cm near the upper part of Half Dome.

Figure 2. The Pathfinder landing site viewed by IMP over an azimuth range of 190° (left) to 275° (right). The mosaic is scaled to match the resolution of the Viking lander cameras (0.7 mrad/pixel). Areas containing abundant ventifacts on rocks are indicated by single-sided arrows. The trend of grooves on the rocks Flat Top and Flute Top are indicated by double-sided arrows. Wedge and Stump have faceted edges that may have formed by aeolian abrasion. Hints of additional flutes are apparent on other rocks, but their true nature cannot be discerned at this resolution.

Figure 3. A comparison between raw Pathfinder IMP (left, 1 mrad/pixel) and Viking Lander 2 (right, 0.7 mrad/pixel) rocks with ventifact-like features. The large, foreground rocks in both images are 24 cm across. Even with the coarse resolution of IMP, flutes can be seen on the foreground rock (Grommit). The VL 2 frame (21B021) shows some of the best examples of aeolian abrasion features at either Viking site. Although elongated pits are visible, no flutes such as those seen on Grommit or those visible on rocks in other IMP images (Figures 1 and 2) are apparent.

Figure 4. Schematic map of the Pathfinder landing site showing ventifacted rocks discussed in this paper. North is to the top and coordinate axes are in meters. Rocks shown as black ovals and labeled in bold print were analyzed by Sojourner's alpha proton x-ray spectrometer. Crosses and labels in normal font show the location of other rocks. Dark lines delineate the rover traverse path (also refer to maps by *Golombek et al.* [this issue]).

Plate 1a. Polar projection showing trends and plunges of flutes at the Pathfinder landing site. The circumferential axis represents trend and the radial axis plunge. Plunges are oriented downward toward the center of the plot and increase inward. Colored symbols correspond to the rocks upon which the flutes are located. Colored lines projecting outward from the edge of the plot show the direction the rover cameras were pointed when images used to derive flute orientations were taken (e.g., for the Moe observations, the rover had a heading of 271°). The association between the rock and rover orientation symbols is shown in the legend at right. The orange arrows represent the range of trends of groove-like features on the surface of Flat Top, as determined from IMP images projected to a bird's eye view using the Ames MarsMap virtual reality system [*Stoker et al.*, 1997]. Solid black arrows are minimum, average, and maximum values of local wind tail directions [*Greeley et al.*, 1997; *Smith et al.*, 1997a]. Arrow with large dashes represents the average trend of wind streaks as seen in orbital images [*Greeley et al.*, 1997; *Smith et al.*, 1997a]. Arrow with small dashes is the predominant wind direction predicted by the General Circulation Model [*Pollack et al.*, 1981; *Greeley et al.*, 1997; *Smith et al.*, 1997a].
Plate 1b. Same as Plate 1a, except showing the mean vector of flutes on each rock.
Plate 1c. Circular normal distribution of flute trends for flutes with azimuths of 180°-360°.

Plate 2. The number of flutes compared to flute dimensions and shape. The color or pattern of the bars corresponds to the rock upon which the flutes are located. (a) Number of measured flutes as a function of length.

Plate 2b. Number of measured flutes as a function of width.

Plate 2c. Number of measured flutes as a function of aspect ratio (length ÷ width).

Plate 3. Flute length versus width. The color or type of symbol corresponds to the rock upon which the flutes are located. Solid diagonal lines are aspect ratios, with values shown in bold type where the lines intersect the plot edge. Areas, assuming a flute shape of an ellipse, are shown as dotted diagonal lines, with values in cm^2 in italic type.

Plate 4. Flute height (the elevation of the middle of the flute above the surface) versus length. The color or type of symbol corresponds to the rock upon which the flutes are located. Because large rocks can have flutes over a range of sizes, as opposed to small rocks which can only have small flutes, only flutes on rocks that are larger than 15 cm are shown. The height of the rocks as seen from the IMP camera is indicated by the horizontal bars (note, portions of the rocks not easily seen by IMP can be higher than these values).

Plate 5a. Flute length versus plunge.
Plate 5b. Flute length versus trend. The solid lines are the minimum, average, and maximum values of local wind tail directions, the line with large dashes represents the average trend of wind streaks as seen in orbital images, and the line with small dashes is the predominant wind direction predicted by the General Circulation Model [*Pollack et al.*, 1981; *Greeley et al.*, 1997; *Smith et al.*, 1997a].

Figure 5. Schematic illustration of the effect of impact angle and rock face orientation on the efficiency of abrasion. Plot from *Greeley et al.* [1982].

Table 1. Flute Orientations

Rock Name	Flute	Trend, deg.[a]	Plunge, deg.[a]	Conf.[b]	Unc. 1, deg.[c]	Method[d]	Unc. 2, deg.[e]	Total Unc., deg.[f]	Res., mm/pix[g]
Casper	1	329	48		4.4	stereo	0.1	5	0.95
Casper	2	322	36		3.2	stereo	0.1	3	0.94
Casper	3	331	59		3.3	stereo	0.1	3	0.94
Casper	4	351	33		1.7	stereo	0.1	2	0.94
Casper	5	333	27		2.3	stereo	0.1	2	0.93
Casper	all	334	41	15					
Ender	1	287	17		1.8	stereo	0.2	2	2.67
Ender	2	315	10		1.3	stereo	0.2	2	2.67
Ender	all	301	14						
Flat Top	1	219/39	12/-12		2.3	interpolation	34	36	1.81
Flat Top	2	329	15		2.1	interpolation	34	36	1.69
Flat Top	all	4	2						
Half Dome	1	282	25		0.4	interpolation	14	14	2.13
Half Dome	2	287	20		0.4	interpolation	14	14	1.80
Half Dome	3	241	27		0.9	interpolation	14	15	2.06
Half Dome	4	283	17		0.6	interpolation	14	15	1.43
Half Dome	all	274	23	23					
Moe	1	287	0		1.1	triangulation	10	11	0.98
Moe	2	288	6		0.8	triangulation	10	11	1.01
Moe	3	309	5		2.0	triangulation	10	12	0.95
Moe	4	307	19		1.2	triangulation	10	11	0.90
Moe	5	297	3		1.0	triangulation	10	11	0.85
Moe	6	255	18		0.3	triangulation	10	10	1.07
Moe	7	290	24		0.9	triangulation	10	11	0.68
Moe	8	305	31		1.6	triangulation	10	12	1.36
Moe	9	278	7		0.7	triangulation	10	11	0.80
Moe	10	305	12		1.2	triangulation	10	11	0.77
Moe	11	265	13		1.7	triangulation	10	12	1.22
Moe	12	247	23		0.5	triangulation	10	11	1.38
Moe	13	199/19	27/-27		2.0	triangulation	10	12	1.25
Moe	14	263	10		0.5	triangulation	10	11	1.03
Moe	15	233	19		0.6	triangulation	10	11	1.00
Moe	16	280	7		0.7	triangulation	10	11	0.78
Moe	17	270	16		0.7	triangulation	10	11	1.05
Moe	18	283	7		0.5	triangulation	10	11	1.22
Moe	19	245	24		1.5	triangulation	10	13	0.92
Moe	20	276	15		0.8	triangulation	10	11	0.79
Moe	all	281	13	13					
Souffle	1	286	26		1.1	monoscopic	0.3	1	1.56
Souffle	all	NA	NA						
Stimpy	1	320	20		0.4	triangulation	14	14	1.21
Stimpy	2	334	15		0.7	triangulation	14	15	1.26
Stimpy	3	289	20		1.5	triangulation	14	16	1.10
Stimpy	4	281	18		1.3	triangulation	14	15	1.07
Stimpy	all	306	20	28					

Rock Name	Flute	Trend, deg.[a]	Plunge, deg.[a]	Conf.[b]	Unc. 1, deg.[c]	Method[d]	Unc. 2, deg.[e]	Total Unc., deg.[f]	Res., mm/pix[g]
Wedge	1	306	13		0.9	interpolation	54	55	1.19
Wedge	2	311	15		0.8	interpolation	54	55	1.39
Wedge	all	309	14	12					
unnamed 1	1	249	11		0.8	stereo	0.4	1	1.75
unnamed 1	2	270	14		0.7	stereo	0.4	1	1.70
unnamed 1	3	247	9		0.6	stereo	0.4	1	1.94
unnamed 1	all	255	12	20					
unnamed 2	1	206	22		1.3	monoscopic	1.6	3	2.14
unnamed 2	all	NA	NA						
unnamed 3	1	322	27		0.8	monoscopic	0.3	1	1.42
unnamed 3	2	157/337 31/-31		1.1		monoscopic	0.3	1	1.36
unnamed 3	3	302	20		1.1	monoscopic	0.3	1	1.49
unnamed 3	all	320	6	61					
unnamed 4	1	310	13		3.1	interpolation	14	17	3.68
unnamed 4	all	NA	NA						
unnamed 5	1	324	31		2.1	monoscopic	0.3	2	1.02
unnamed 5	all	NA	NA						
unnamed 6	1	147	25		1.0	interpolation	37	38	1.26
unnamed 6	2	112	12		1.2	interpolation	37	38	1.21
unnamed 6	all	129	19	87					
unnamed 7	1	223	7		0.7	stereo	0.2	1	1.37
unnamed 7	all	NA	NA						

[a]: Trend and plunges for rows labeled "all" are the mean vector of the flute orientations on a given rock. Plunge is downward away from the trend direction. Where two values are given for trend and plunge, the first is the actual measured value. The second value is oriented 180° from the measured trend and are used to derive the mean vector.

[b]: 95% confidence cone. Where no values are listed, points are too scattered or the mean length is too low to compute a concentration factor.

[c]: The uncertainty of flute orientation within rover images. This applies to both trend and plunge measurements.

[d]: The method to determine rover position.

[e]: The uncertainty of rover position. The computation of this depends upon the method used to determine rover position. See text for details. This applies to the trend measurement.

[f]: Uncertainty 1 + Uncertainty 2 (rounded to nearest degree). This applies to the trend measurement.

[g]: Spatial resolution in mm per pixel.

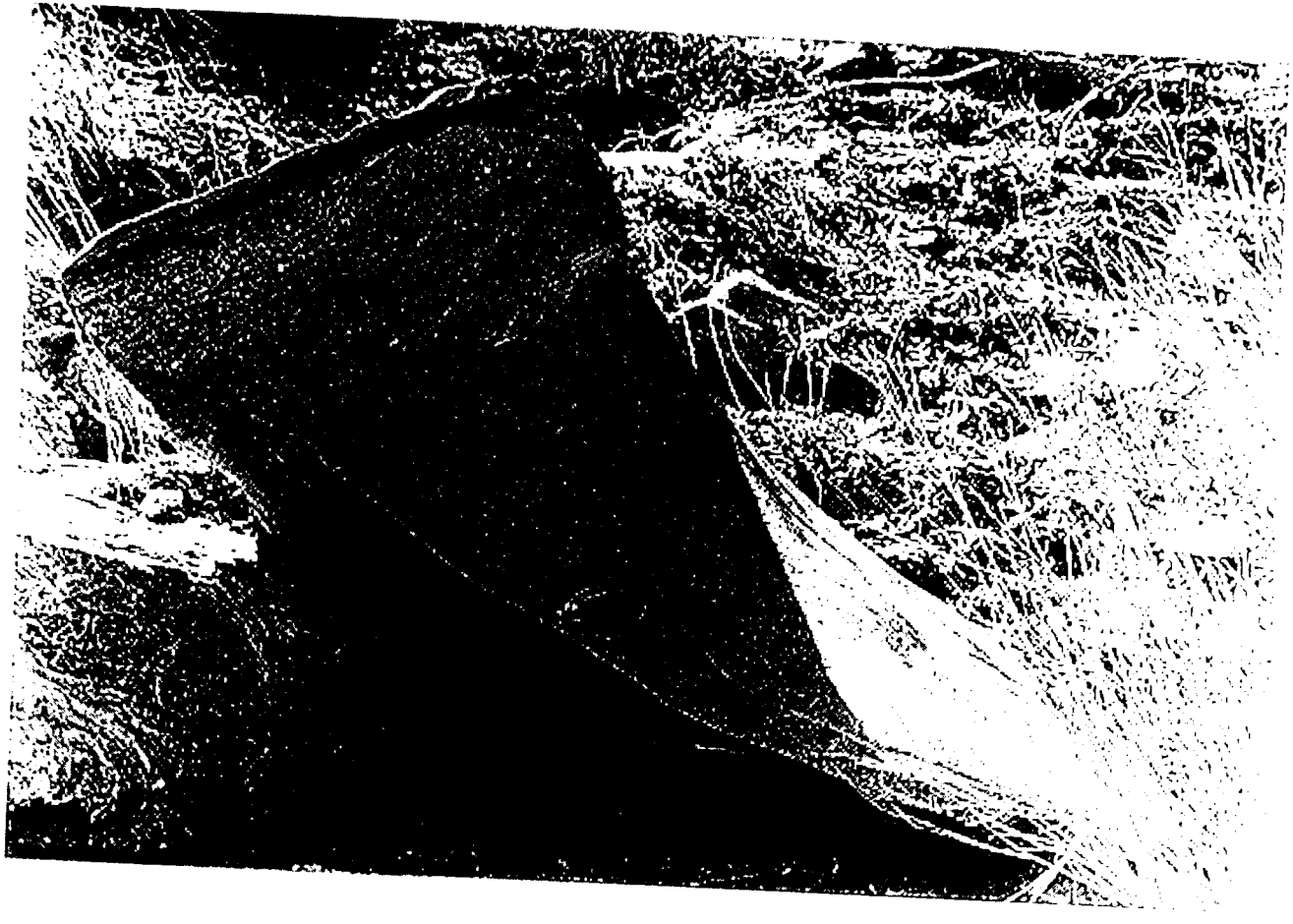

Figure 1a-left

Figure 1a-right

Figure 1b-left

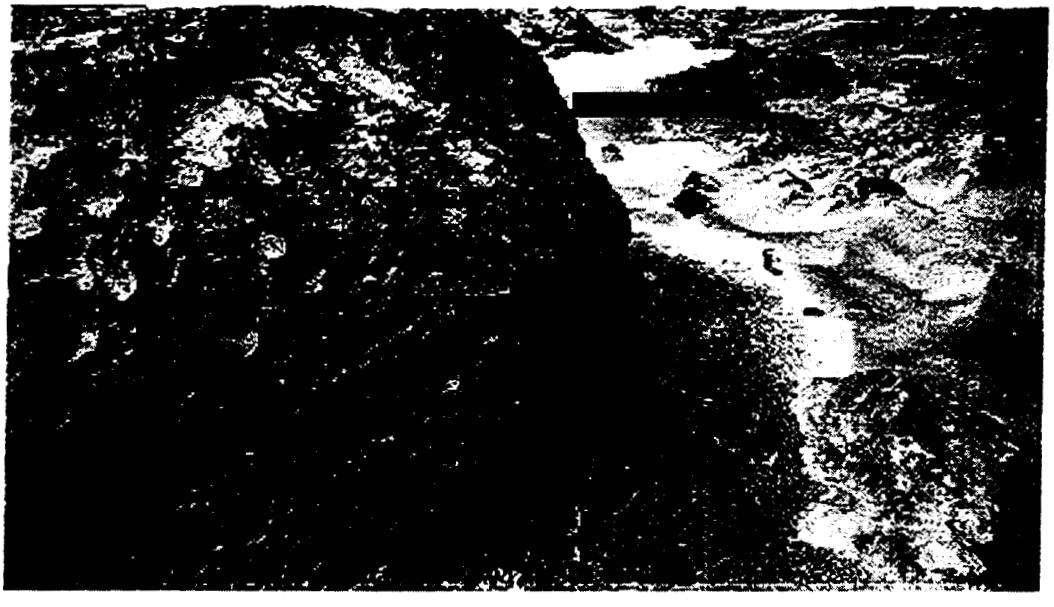

Figure 1b-right

Figure 1c-left

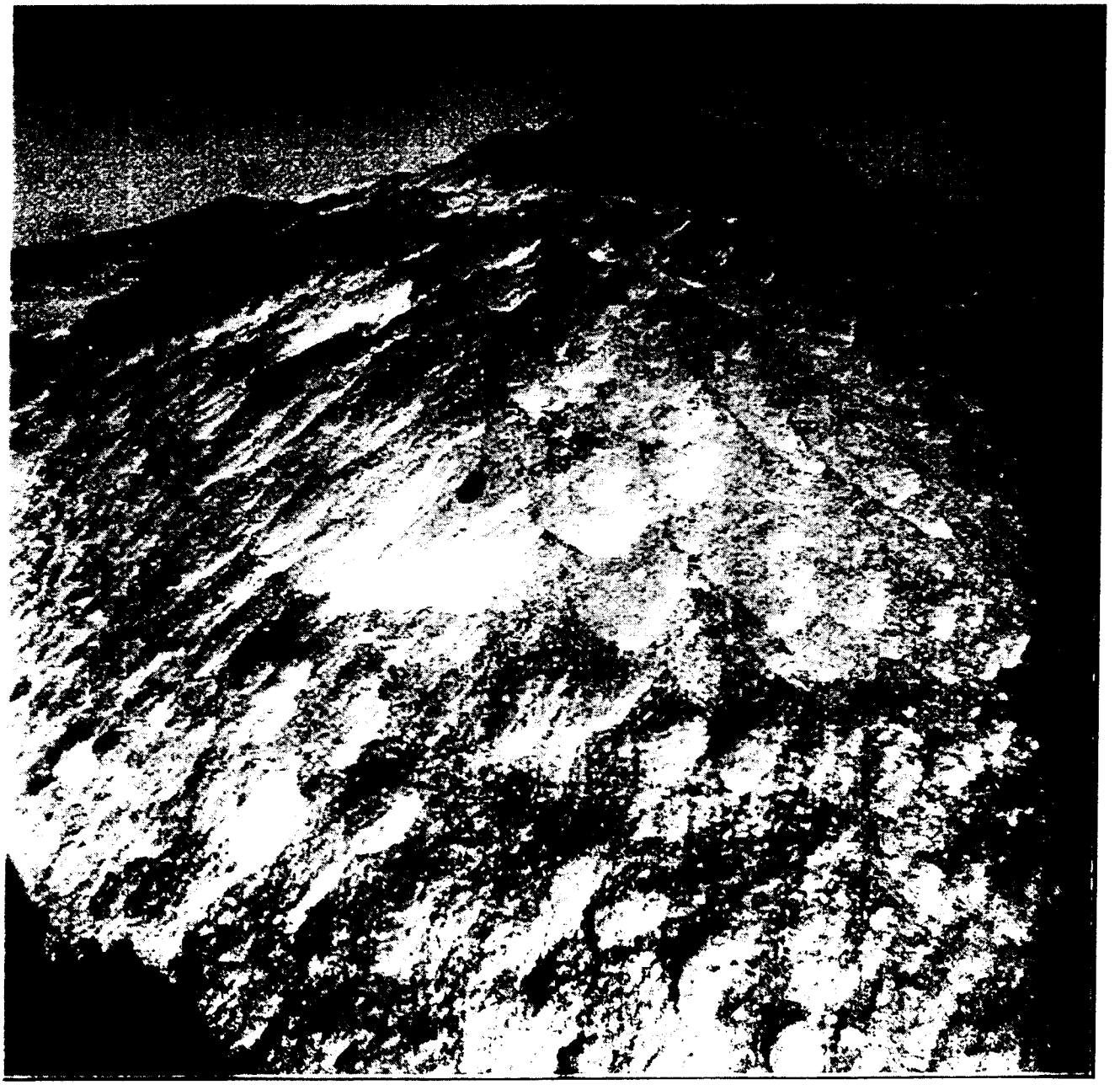

Figure 1c-right

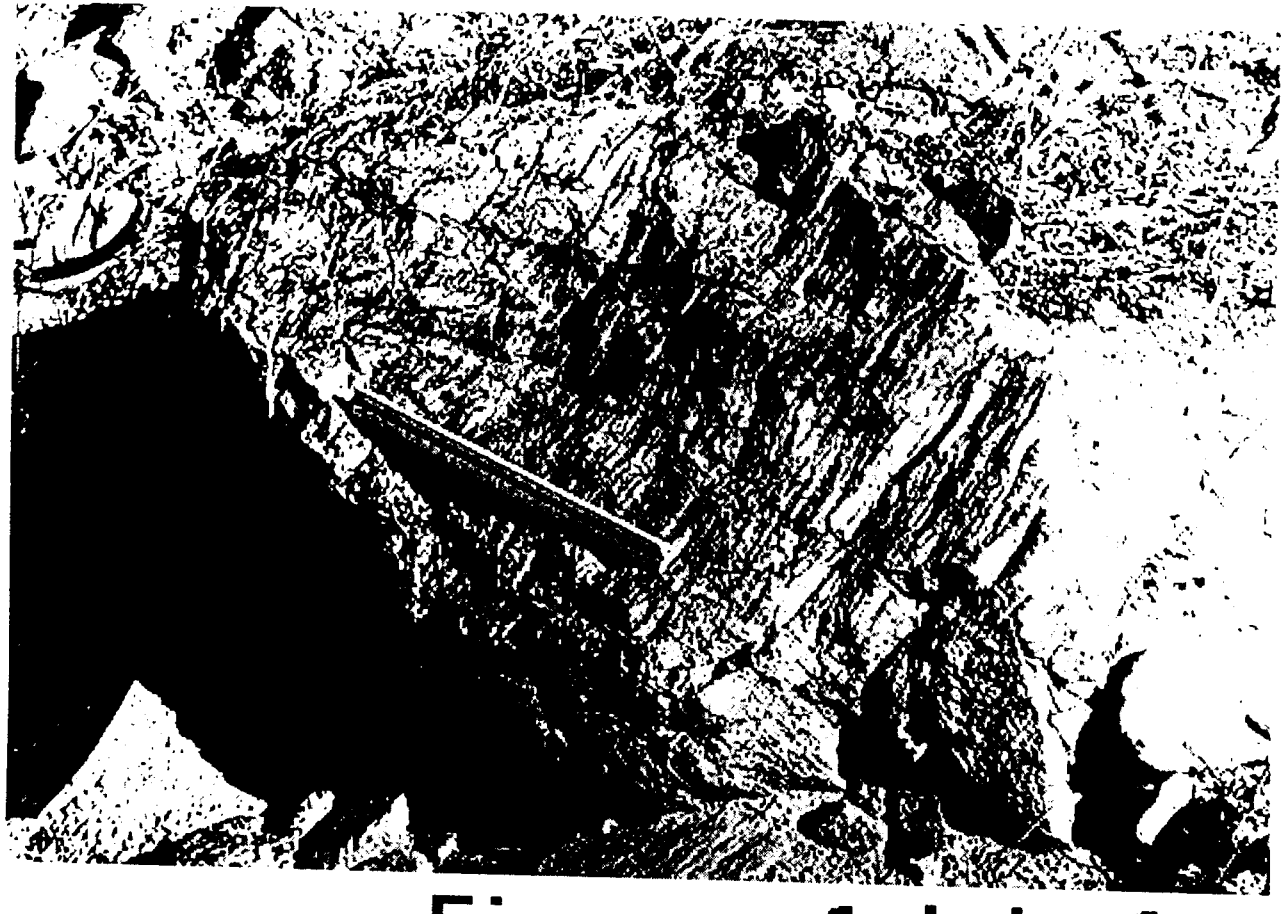

Figure 1d-left

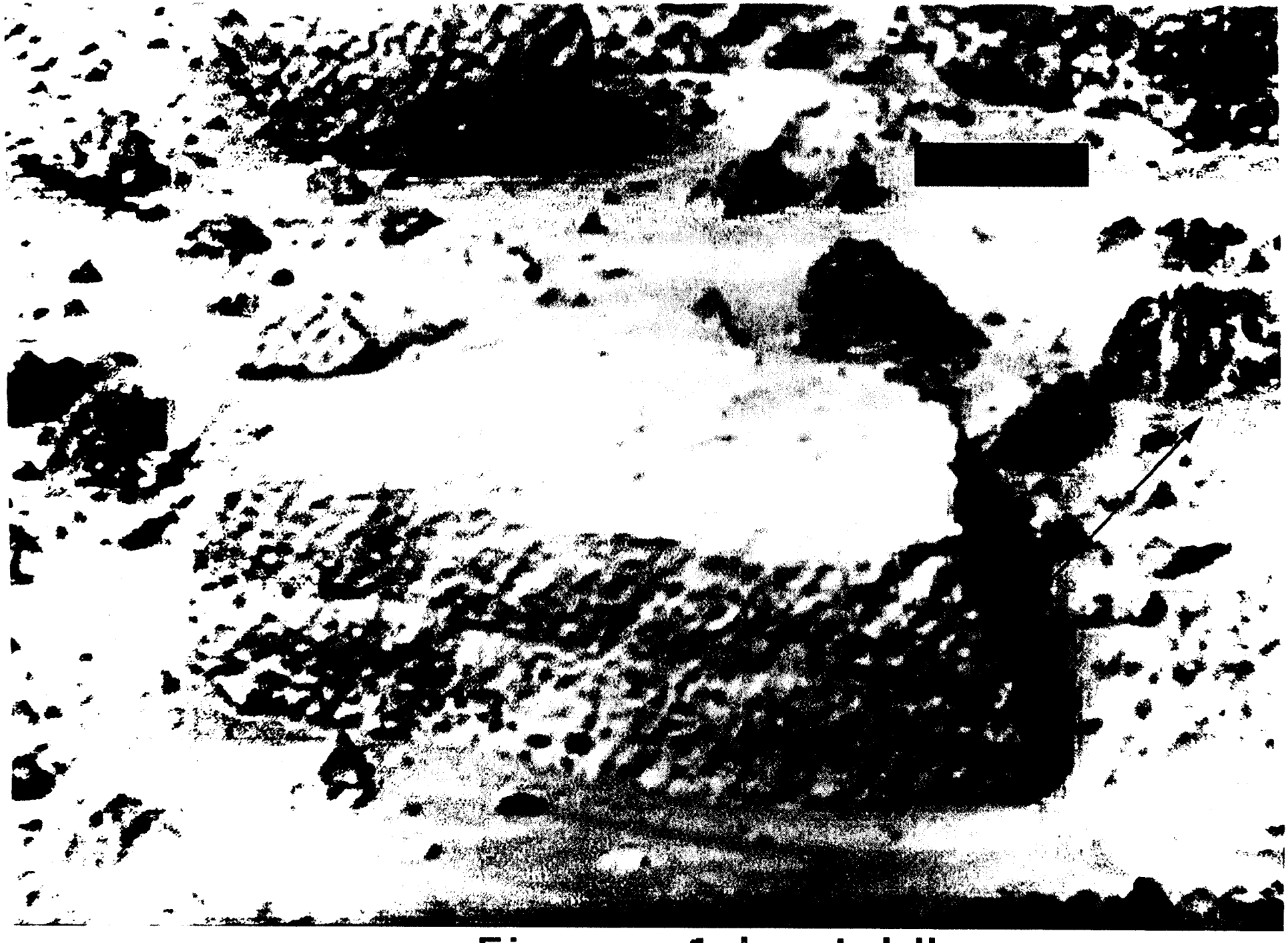

Figure 1d-middle

Figure 1d-right

Figure 1e-left

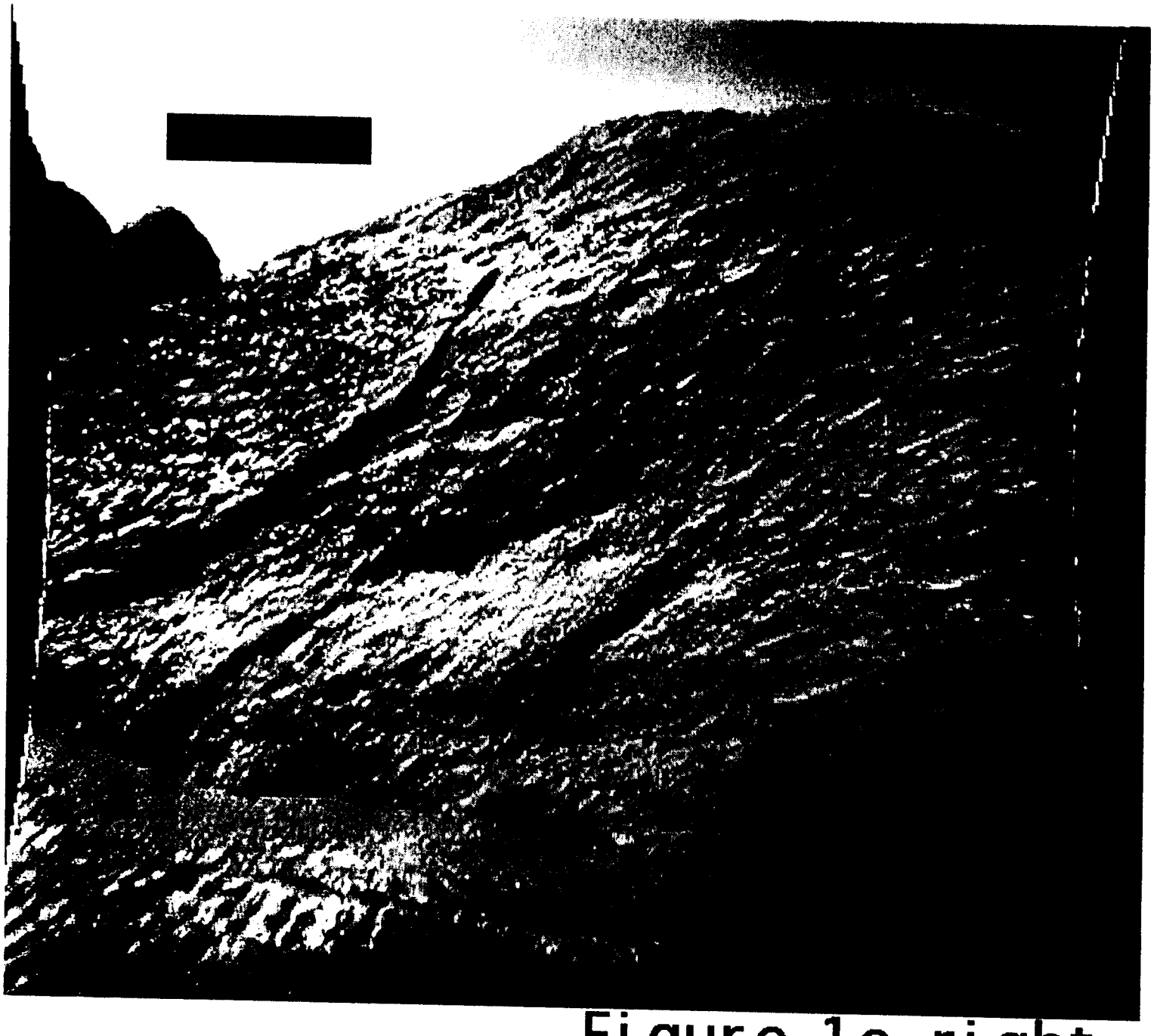

Figure 1e-right

Figure 2

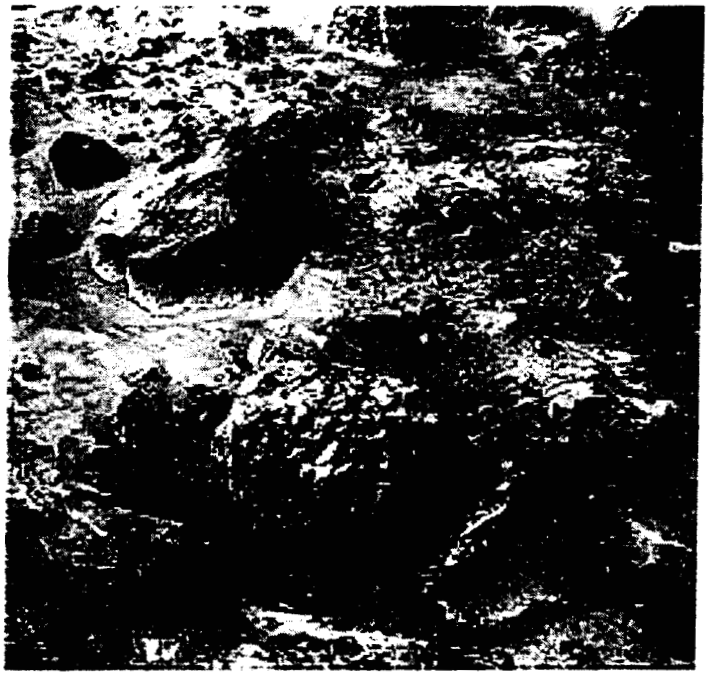

Figure 3-left

Figure 3-right

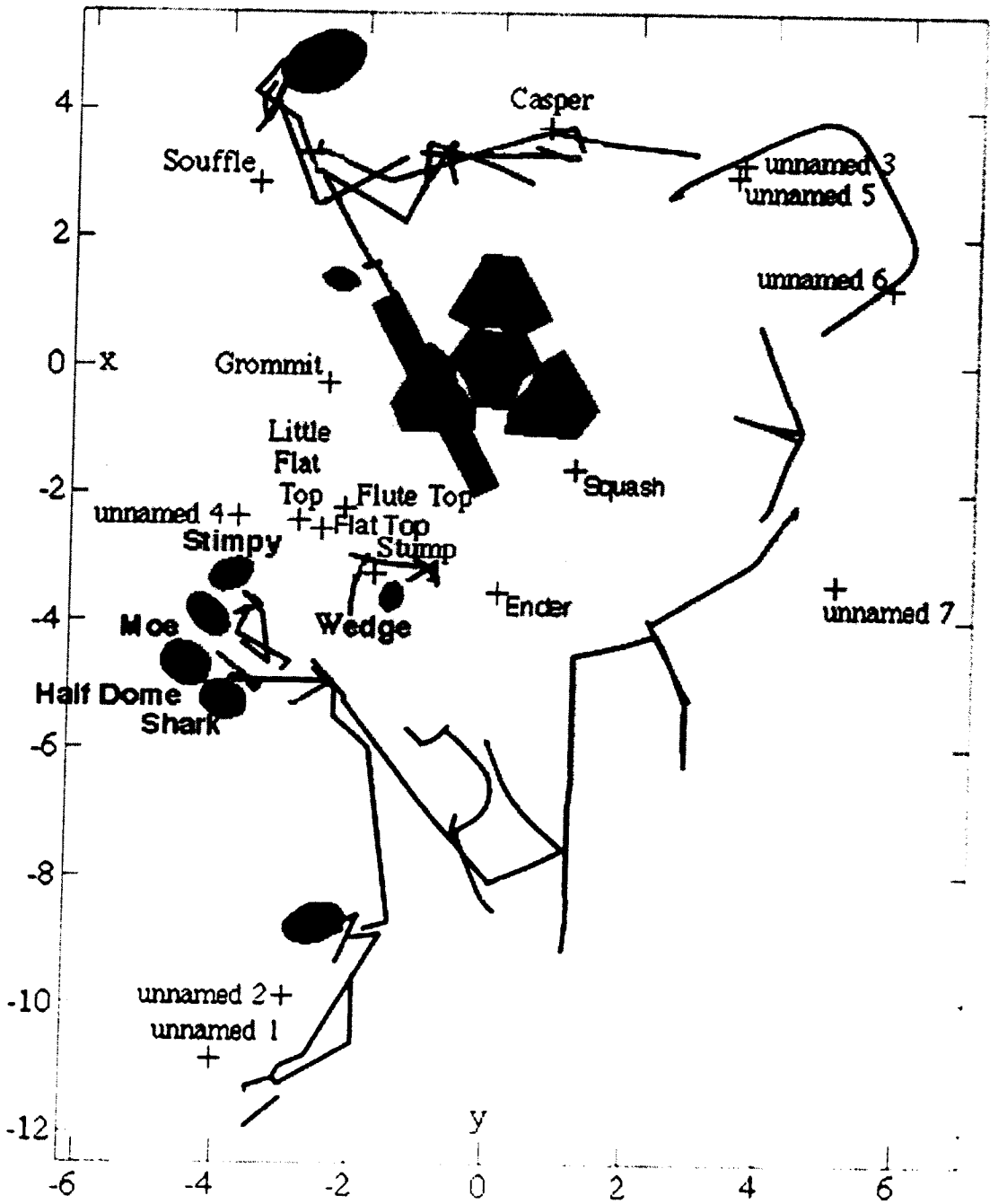
Casper
Souffle
unnamed 3
unnamed 5
unnamed 6
Grommit
Little
Flat
Top
Flute Top
Squash
unnamed 4
Flat Top
Stumpy
Stump
Ender
unnamed 7
Moe
Wedge
Half Dome
Shark
unnamed 2
unnamed 1
x
y
4
2
0
-2
-4
-6
-8
-10
-12
-6
-4
-2
0
2
4
6

Figure 4

ABRASION vs. IMPACT ANGLE

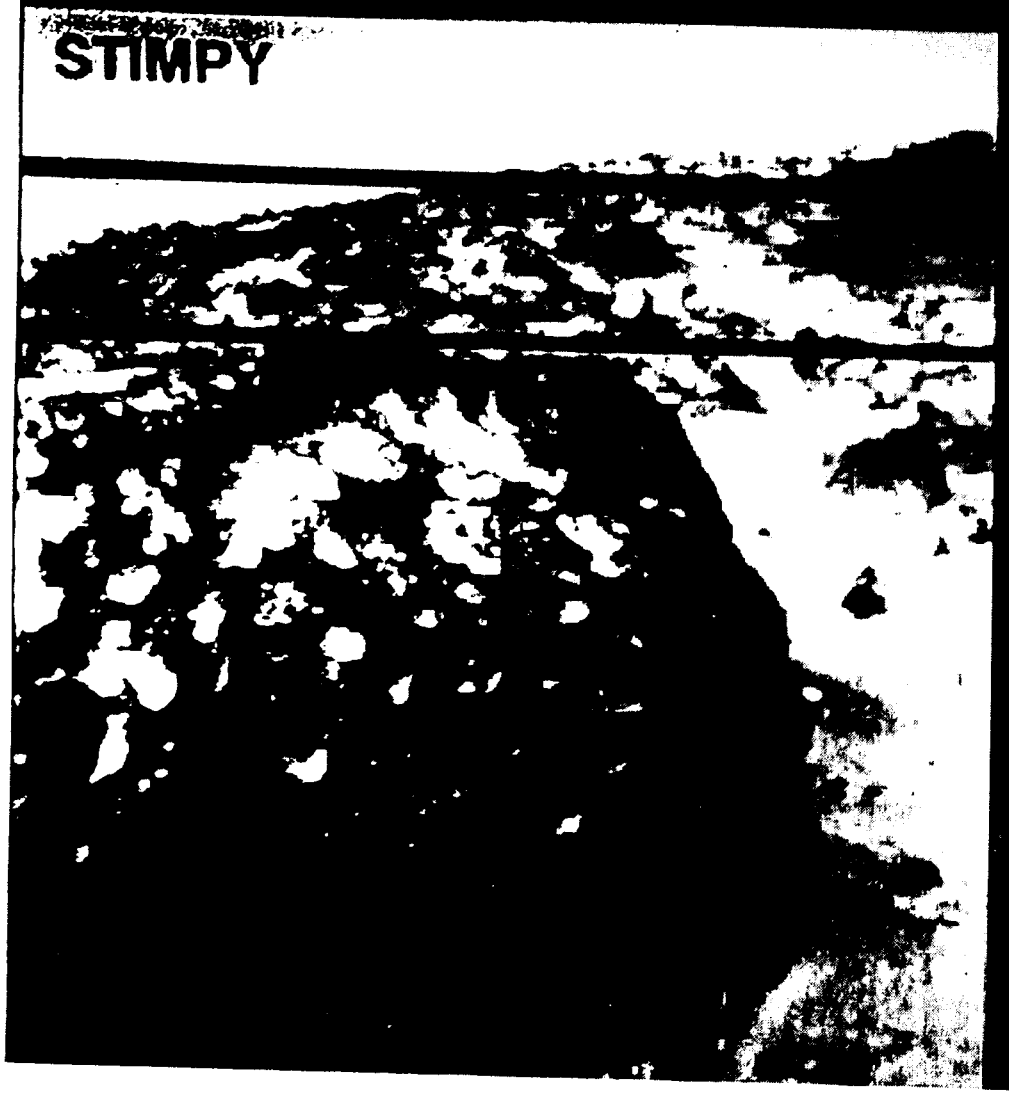

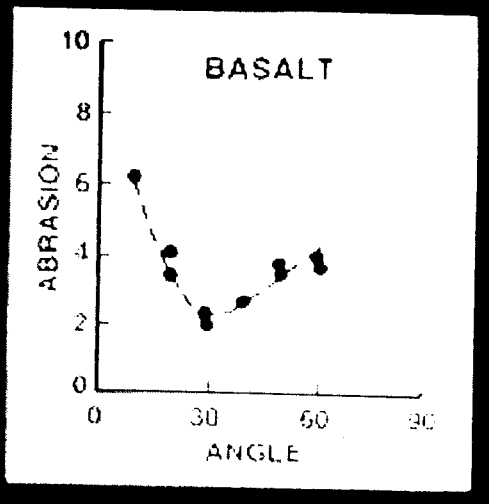

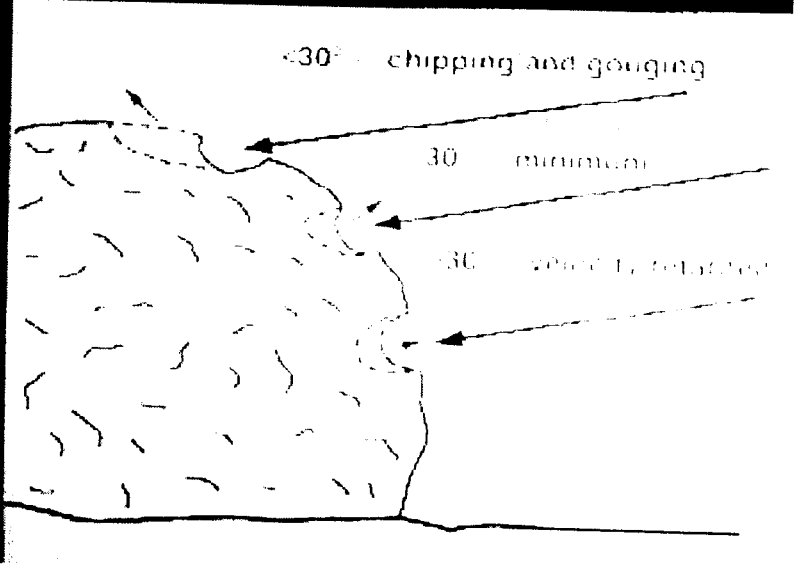

Figure 10

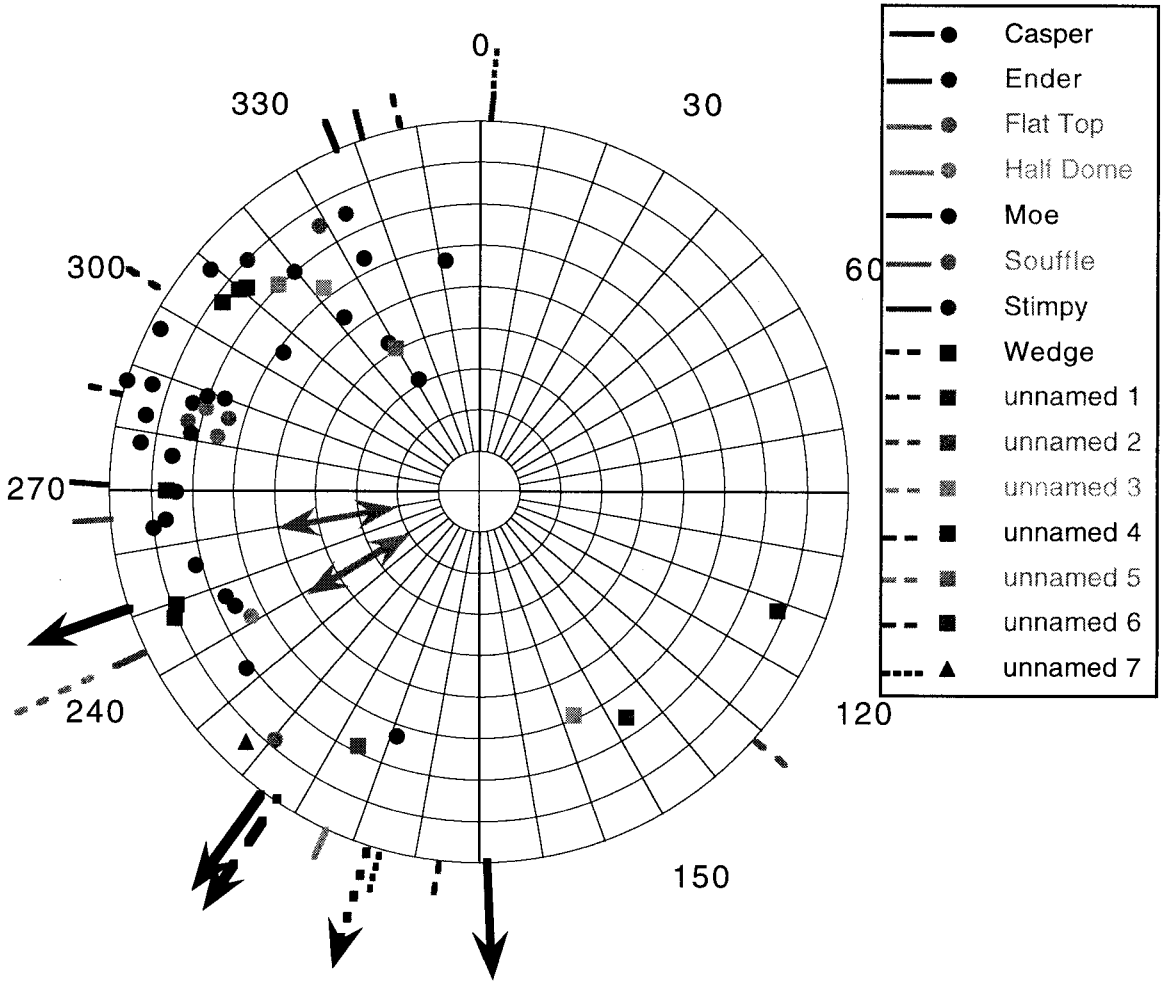
0
30
60
120
150
240
270
300
330
Casper
Ender
Flat Top
Half Dome
Moe
Souffle
Stimpy
Wedge
unnamed 1
unnamed 2
unnamed 3
unnamed 4
unnamed 5
unnamed 6
unnamed 7

Plate 19

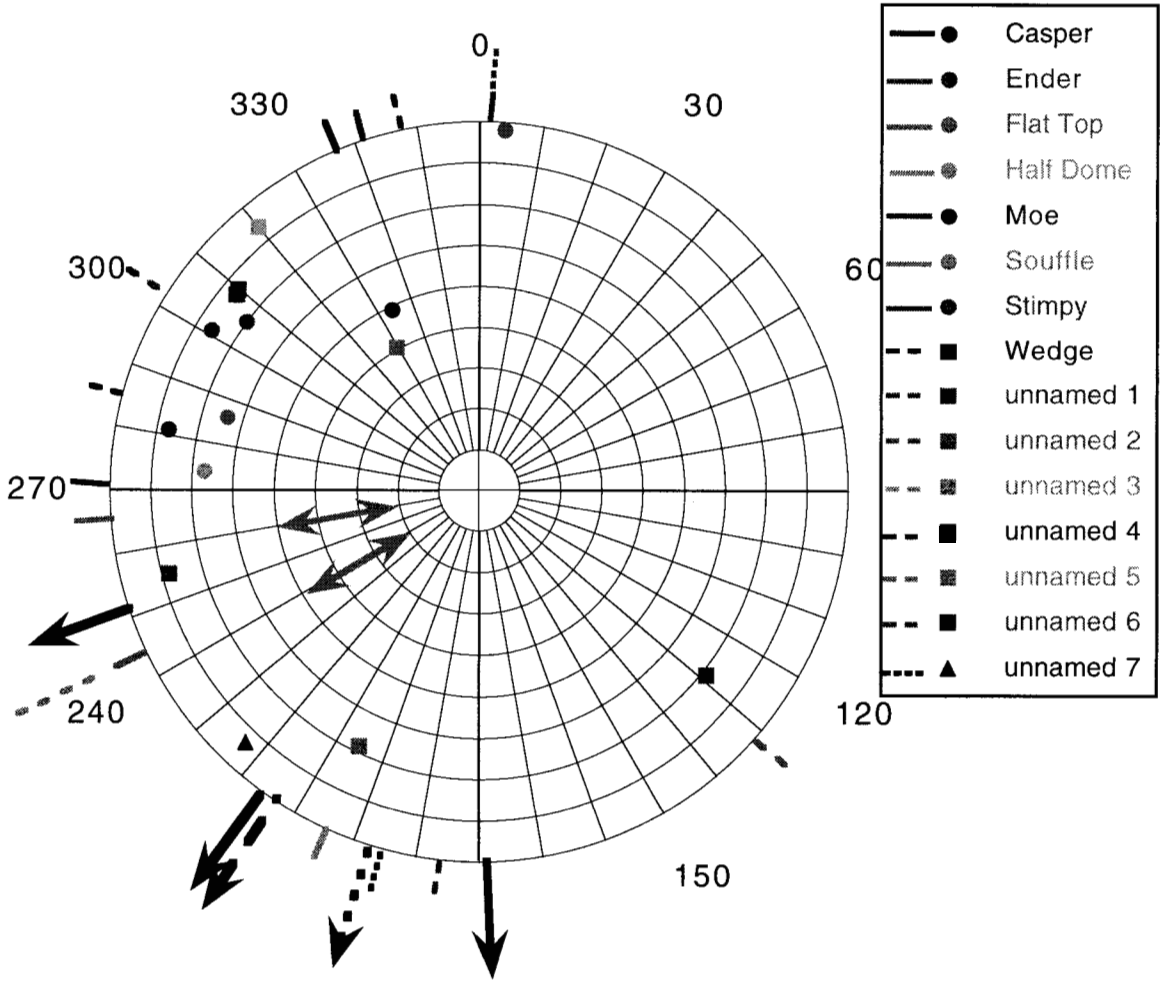
0
30
60
120
150
240
270
300
330
Casper
Ender
Flat Top
Half Dome
Moe
Souffle
Stimpy
Wedge
unnamed 1
unnamed 2
unnamed 3
unnamed 4
unnamed 5
unnamed 6
unnamed 7

Plate 16

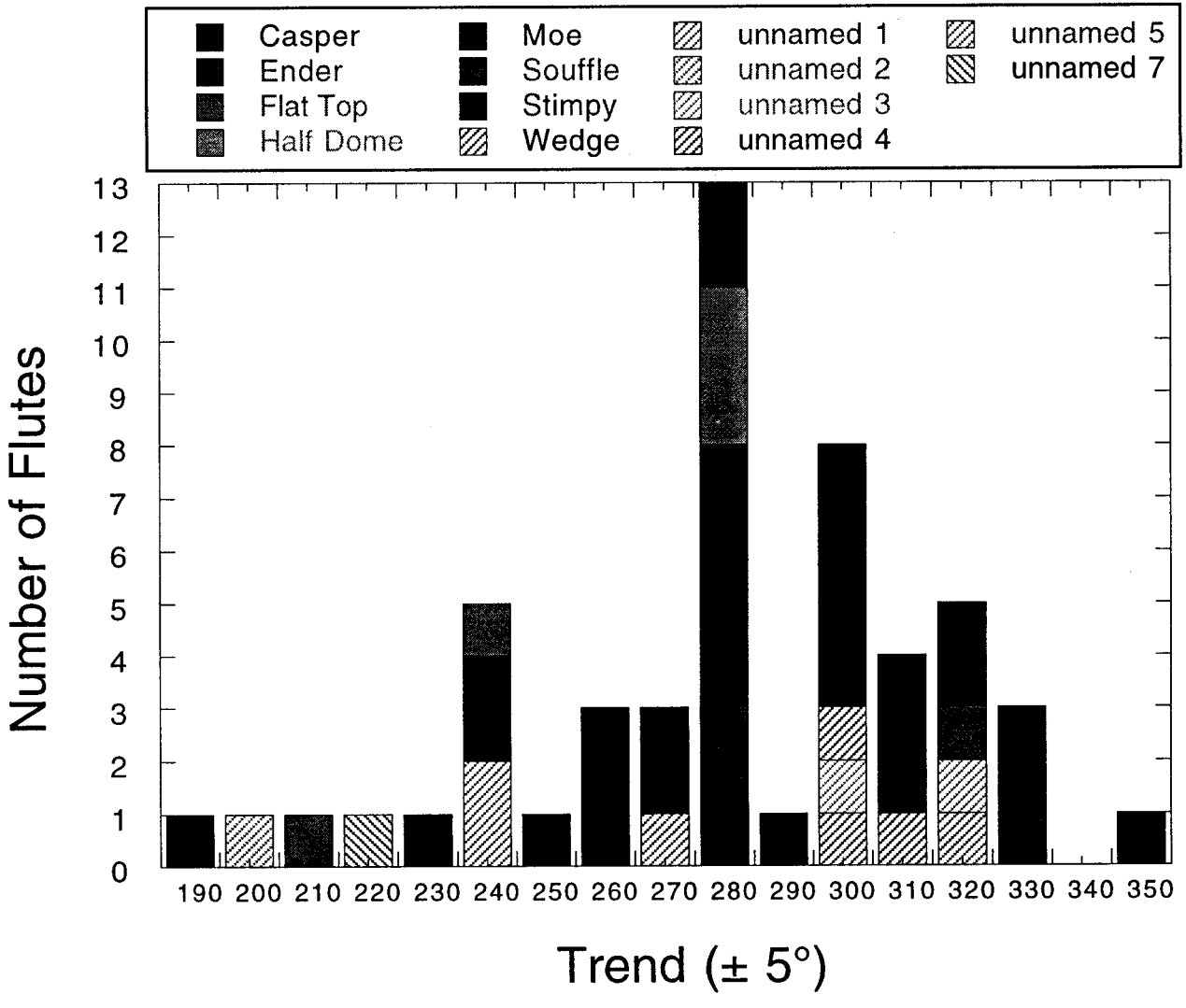
Casper
Ender
Flat Top
Half Dome
Moe
Souffle
Stimpy
Wedge
unnamed 1
unnamed 2
unnamed 3
unnamed 4
unnamed 5
unnamed 7
Number of Flutes
0
1
2
3
4
5
6
7
8
9
10
11
12
13
190 200 210 220 230 240 250 260 270 280 290 300 310 320 330 340 350
Trend (± 5°)

Plate 1C

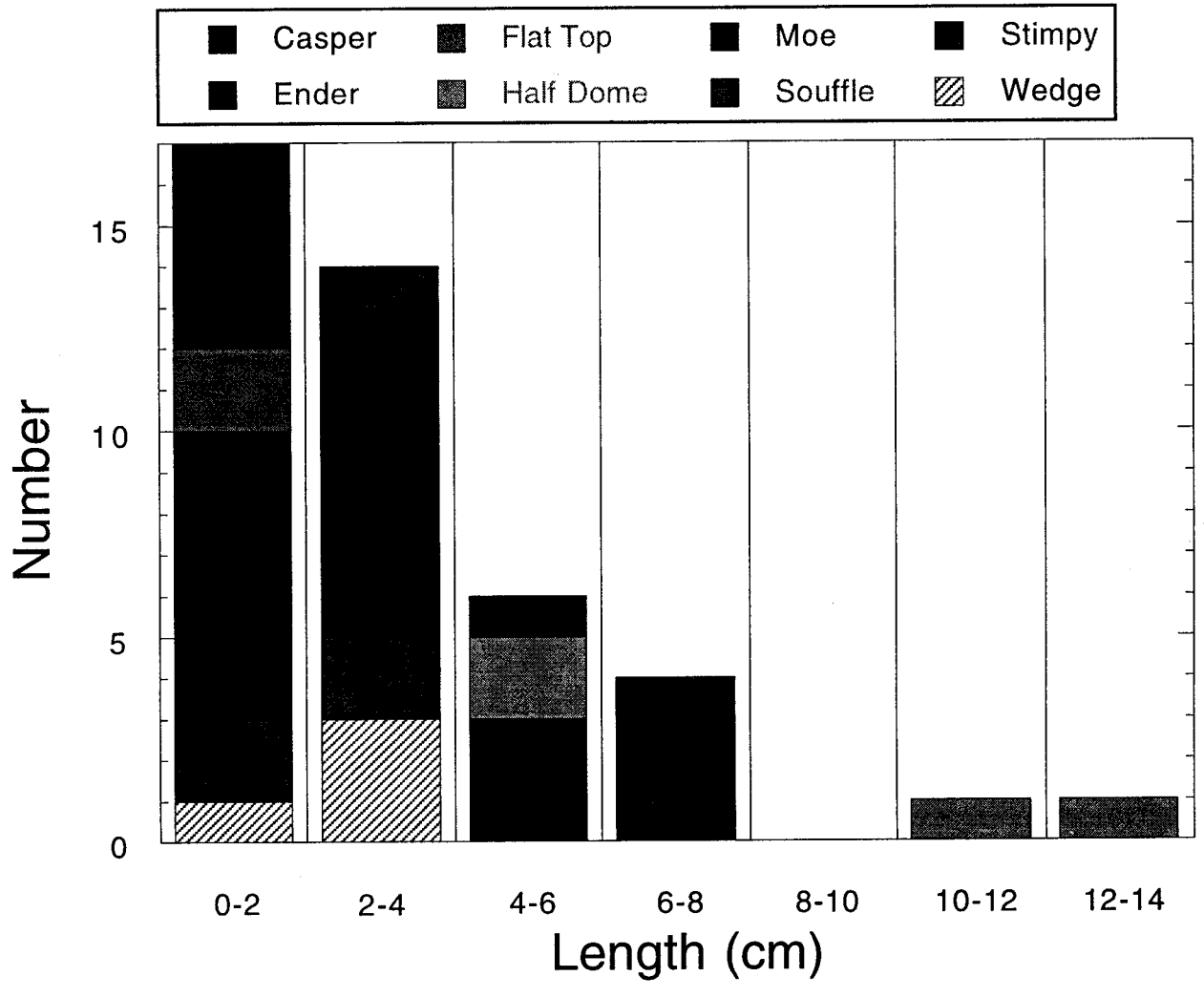
Casper
Ender
Flat Top
Half Dome
Moe
Souffle
Stimpy
Wedge
Number
15
10
5
0
0-2
2-4
4-6
6-8
8-10
10-12
12-14
Length (cm)

Plate 2a

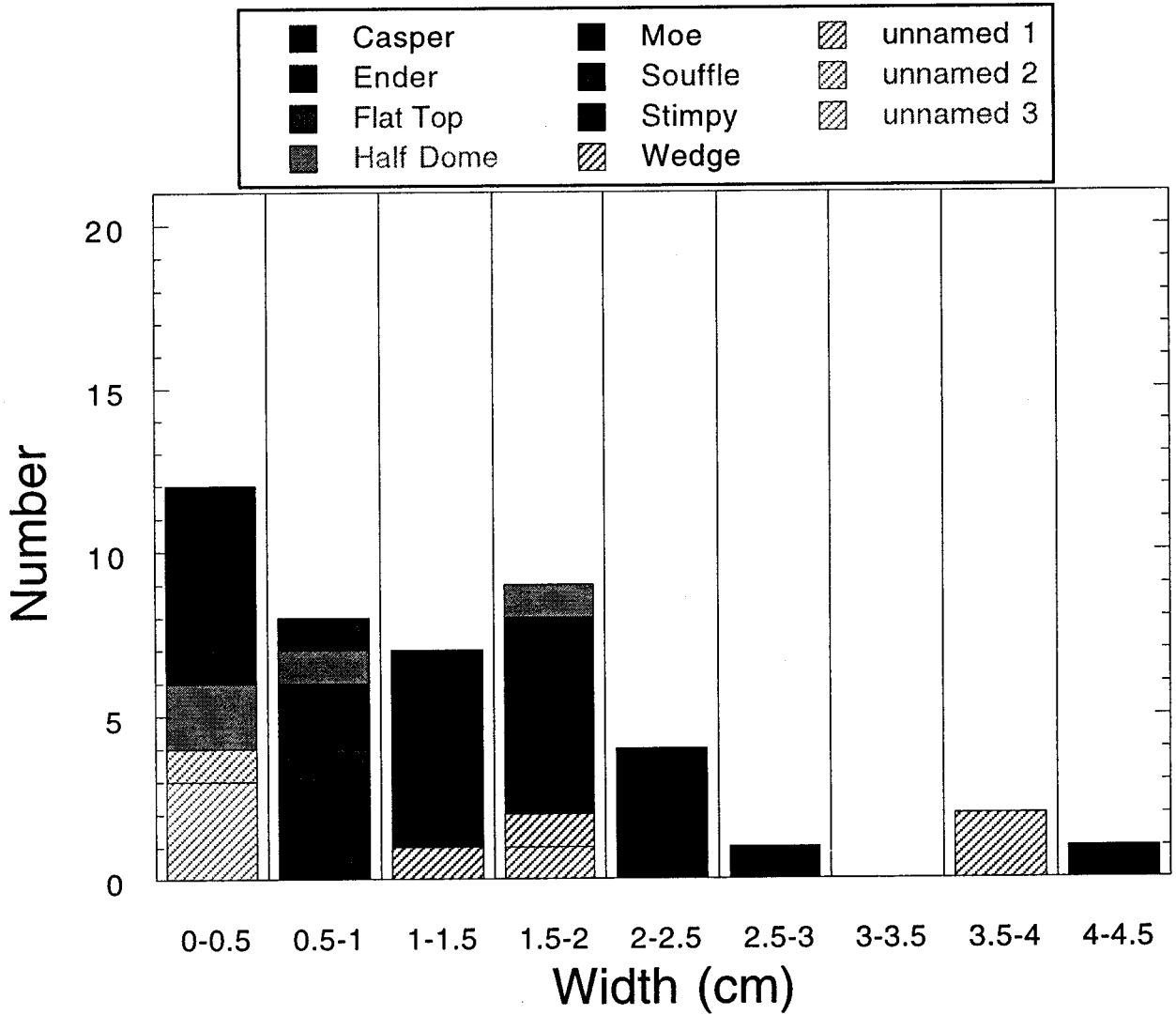
Casper
Ender
Flat Top
Half Dome
Moe
Souffle
Stimpy
Wedge
unnamed 1
unnamed 2
unnamed 3
Number
0
5
10
15
20
0-0.5
0.5-1
1-1.5
1.5-2
2-2.5
2.5-3
3-3.5
3.5-4
4-4.5
Width (cm)

Plate 26

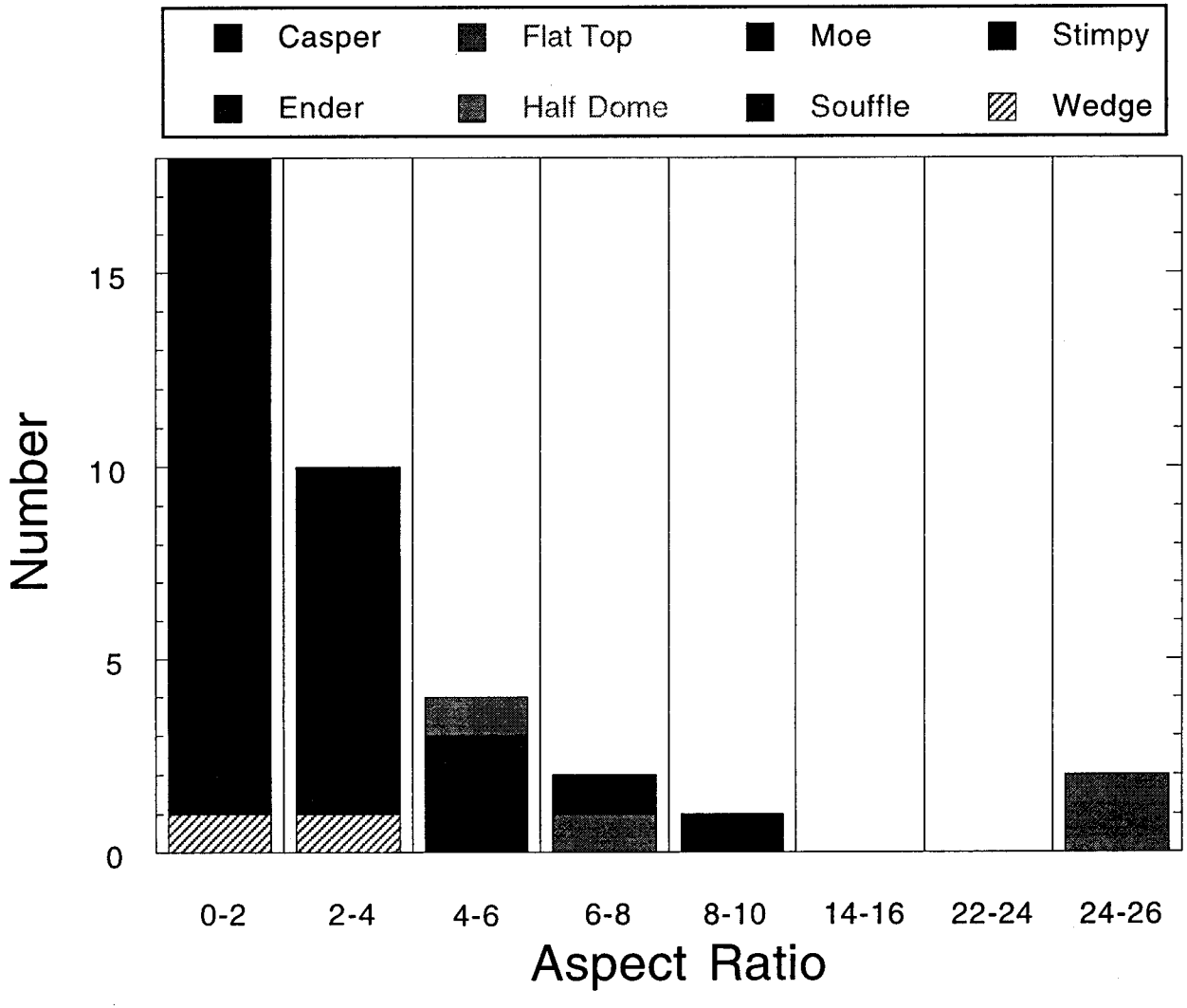
Casper
Flat Top
Moe
Stimpy
Ender
Half Dome
Souffle
Wedge
Number
15
10
5
0
0-2
2-4
4-6
6-8
8-10
14-16
22-24
24-26
Aspect Ratio

Plate 2C

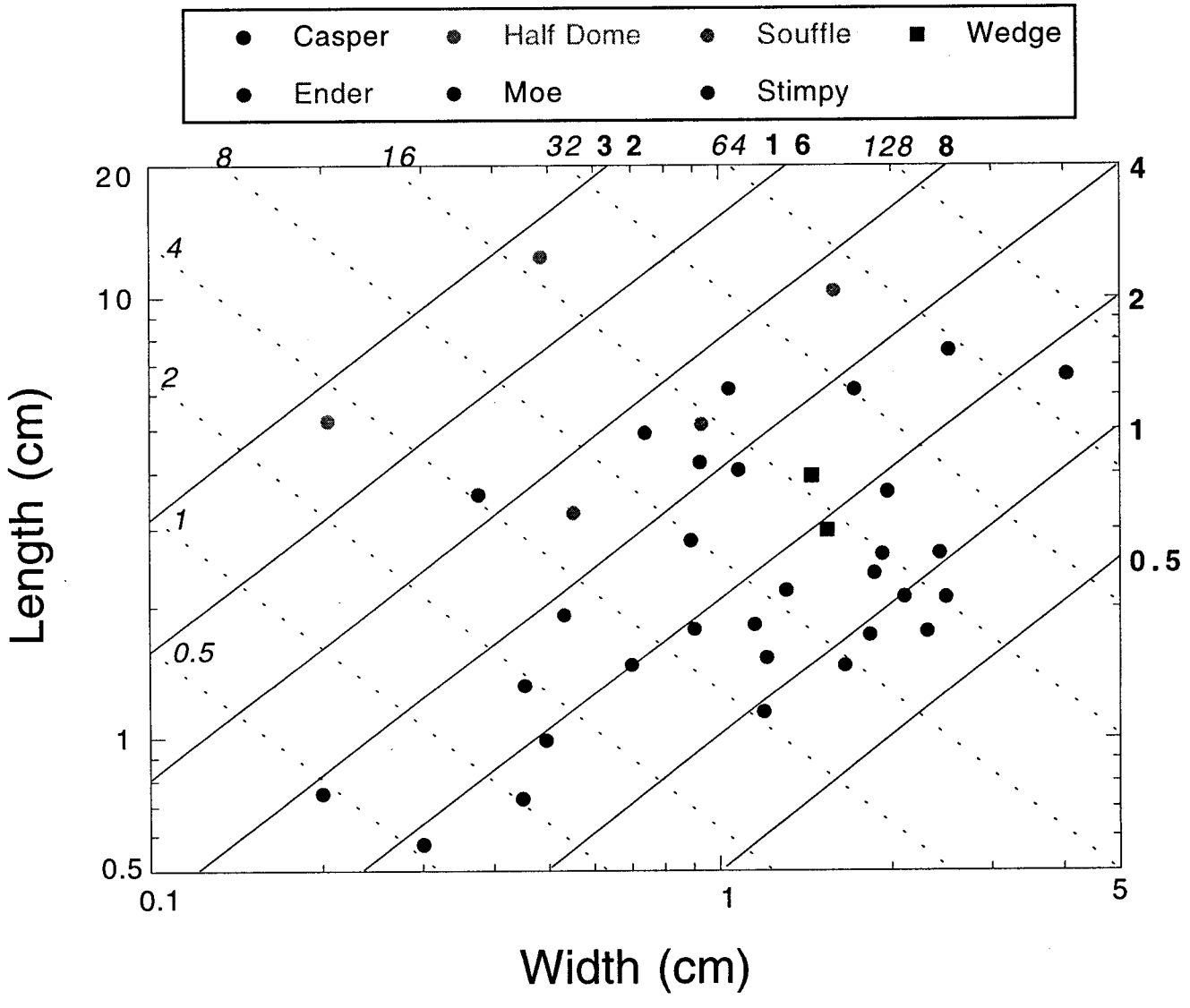
Casper
Half Dome
Souffle
Wedge
Ender
Moe
Stimpy
8
16
32
3 2
64
1 6
128
8
4
2
1
0.5
20
10
1
0.5
4
2
1
0.5
0.1
1
5
Length (cm)
Width (cm)

Plate 9

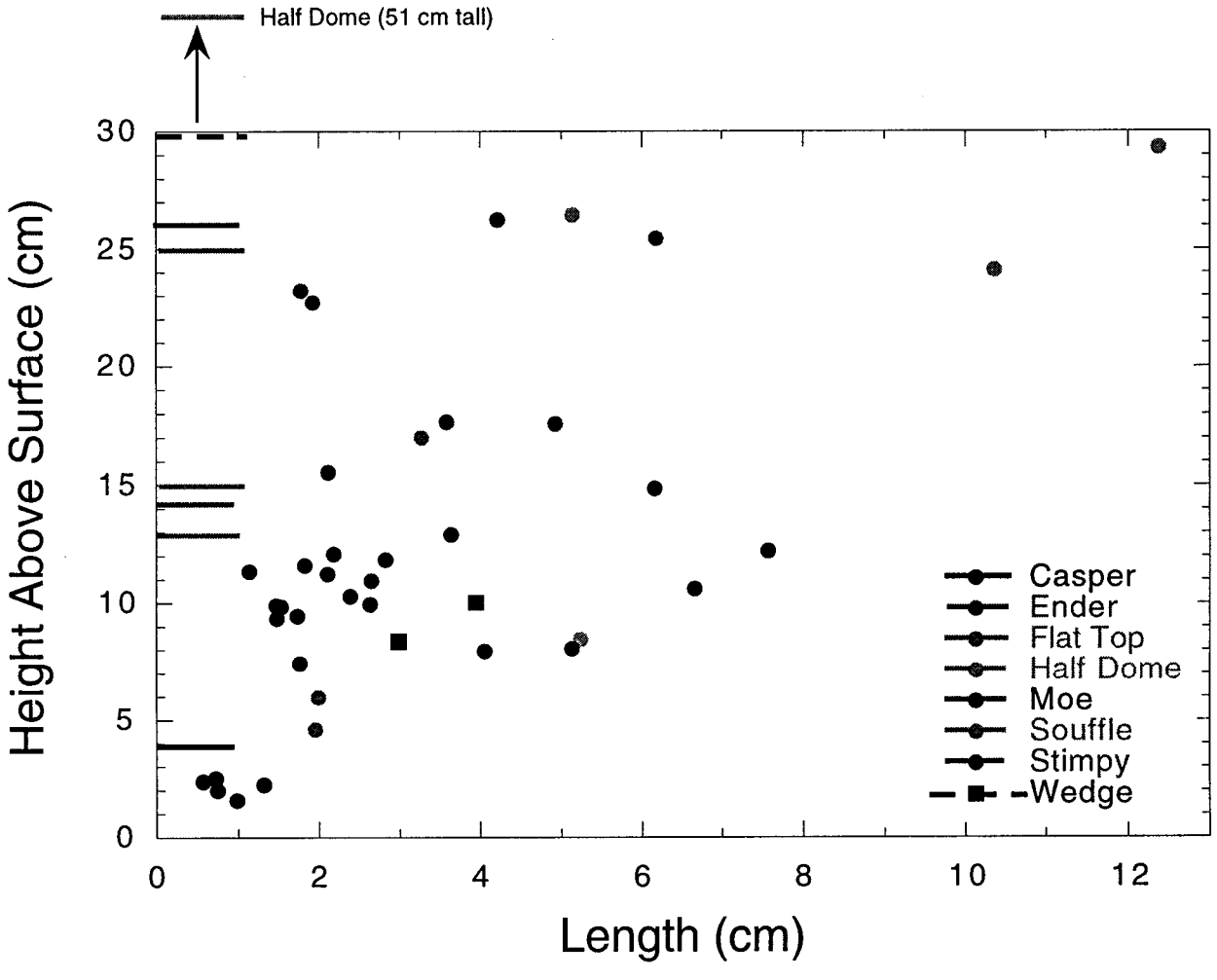
Half Dome (51 cm tall)
Height Above Surface (cm)
Length (cm)
0
5
10
15
20
25
30
0
2
4
6
8
10
12
Casper
Ender
Flat Top
Half Dome
Moe
Souffle
Stimpy
Wedge

plate 4

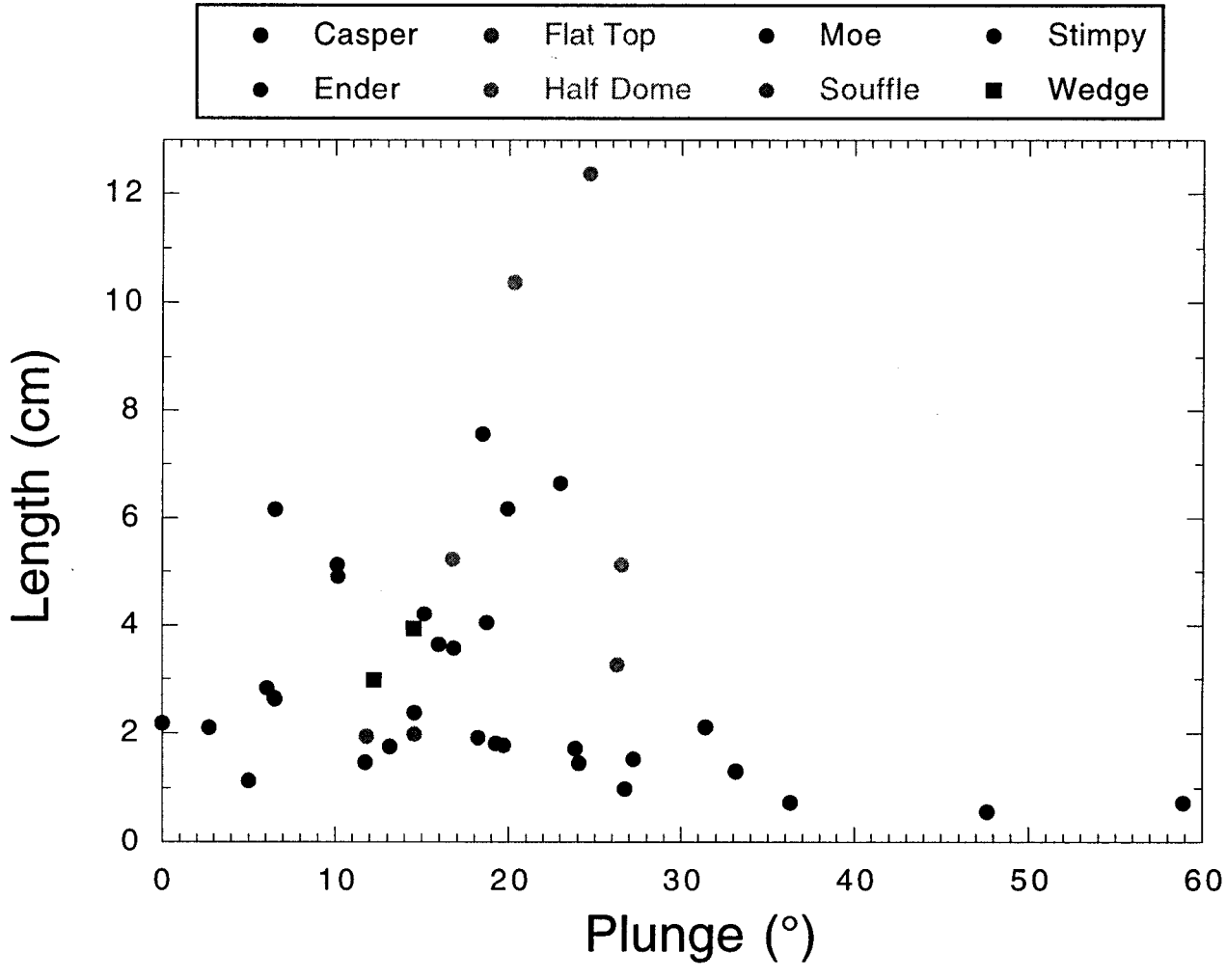
Casper
Flat Top
Moe
Stimpy
Ender
Half Dome
Souffle
Wedge
Length (cm)
0
2
4
6
8
10
12
0
10
20
30
40
50
60
Plunge (°)

Plate 9a

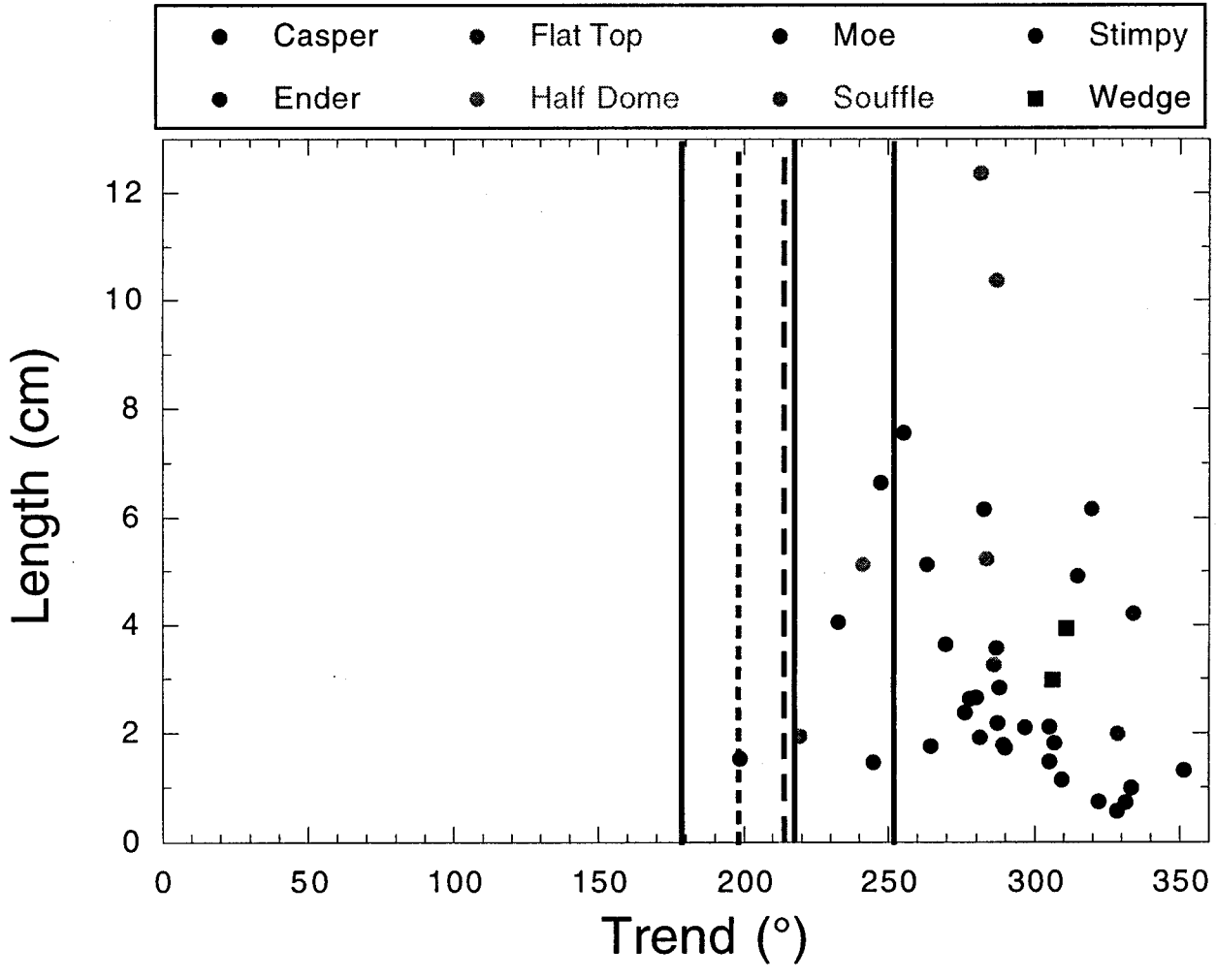
Casper
Flat Top
Moe
Stimpy
Ender
Half Dome
Souffle
Wedge
Length (cm)
0
2
4
6
8
10
12
0
50
100
150
200
250
300
350
Trend (°)

Plate 5b

N. T. Bridges, A. F. C. Haldemann, K. E. Herkenhoff, and T. J. Parker, Jet Propulsion Laboratory, MS 183-501, 4800 Oak Grove Drive, Pasadena, CA 91109 (nathan.bridges@jpl.nasa.gov)
R. Greeley and M. Kraft, Department of Geology, Arizona State University, Tempe, AZ 85287
A. W. Ward, U.S. Geological Survey, Flagstaff, AZ 86001

---

[1] Jet Propulsion Laboratory, California Institute of Technology, Pasadena, California

[2] Department of Geology, Arizona State University, Tempe, Arizona

[3] U.S. Geological Survey, Flagstaff, Arizona

[4] Now at U.S. Geological Survey, Flagstaff, Arizona

(Received March 25, 1998; revised July 7, 1998; accepted July 17, 1998.)

Paper 98JE02550
0148-0227/98/98JE-02550$09.00

BRIDGES ET AL.: PATHFINDER VENTIFACTS

BRIDGES ET AL.: PATHFINDER VENTIFACTS

BRIDGES ET AL.: PATHFINDER VENTIFACTS

BRIDGES ET AL.: PATHFINDER VENTIFACTS

BRIDGES ET AL.: PATHFINDER VENTIFACTS

BRIDGES ET AL.: PATHFINDER VENTIFACTS

BRIDGES ET AL.: PATHFINDER VENTIFACTS

BRIDGES ET AL.: PATHFINDER VENTIFACTS

BRIDGES ET AL.: PATHFINDER VENTIFACTS

BRIDGES ET AL.: PATHFINDER VENTIFACTS

BRIDGES ET AL.: PATHFINDER VENTIFACTS

BRIDGES ET AL.: PATHFINDER VENTIFACTS

BRIDGES ET AL.: PATHFINDER VENTIFACTS

BRIDGES ET AL.: PATHFINDER VENTIFACTS

BRIDGES ET AL.: PATHFINDER VENTIFACTS

BRIDGES ET AL.: PATHFINDER VENTIFACTS

BRIDGES ET AL.: PATHFINDER VENTIFACTS

BRIDGES ET AL.: PATHFINDER VENTIFACTS

BRIDGES ET AL.: PATHFINDER VENTIFACTS

BRIDGES ET AL.: PATHFINDER VENTIFACTS

BRIDGES ET AL.: PATHFINDER VENTIFACTS

BRIDGES ET AL.: PATHFINDER VENTIFACTS

BRIDGES ET AL.: PATHFINDER VENTIFACTS

BRIDGES ET AL.: PATHFINDER VENTIFACTS

BRIDGES ET AL.: PATHFINDER VENTIFACTS

BRIDGES ET AL.: PATHFINDER VENTIFACTS
BRIDGES ET AL.: PATHFINDER VENTIFACTS
BRIDGES ET AL.: PATHFINDER VENTIFACTS
BRIDGES ET AL.: PATHFINDER VENTIFACTS
BRIDGES ET AL.: PATHFINDER VENTIFACTS
BRIDGES ET AL.: PATHFINDER VENTIFACTS
BRIDGES ET AL.: PATHFINDER VENTIFACTS
BRIDGES ET AL.: PATHFINDER VENTIFACTS
BRIDGES ET AL.: PATHFINDER VENTIFACTS
BRIDGES ET AL.: PATHFINDER VENTIFACTS
BRIDGES ET AL.: PATHFINDER VENTIFACTS
BRIDGES ET AL.: PATHFINDER VENTIFACTS
BRIDGES ET AL.: PATHFINDER VENTIFACTS
BRIDGES ET AL.: PATHFINDER VENTIFACTS
BRIDGES ET AL.: PATHFINDER VENTIFACTS
BRIDGES ET AL.: PATHFINDER VENTIFACTS
BRIDGES ET AL.: PATHFINDER VENTIFACTS
BRIDGES ET AL.: PATHFINDER VENTIFACTS
BRIDGES ET AL.: PATHFINDER VENTIFACTS
BRIDGES ET AL.: PATHFINDER VENTIFACTS
BRIDGES ET AL.: PATHFINDER VENTIFACTS
BRIDGES ET AL.: PATHFINDER VENTIFACTS
BRIDGES ET AL.: PATHFINDER VENTIFACTS
BRIDGES ET AL.: PATHFINDER VENTIFACTS
BRIDGES ET AL.: PATHFINDER VENTIFACTS
BRIDGES ET AL.: PATHFINDER VENTIFACTS
BRIDGES ET AL.: PATHFINDER VENTIFACTS
BRIDGES ET AL.: PATHFINDER VENTIFACTS
BRIDGES ET AL.: PATHFINDER VENTIFACTS
BRIDGES ET AL.: PATHFINDER VENTIFACTS
BRIDGES ET AL.: PATHFINDER VENTIFACTS
BRIDGES ET AL.: PATHFINDER VENTIFACTS
BRIDGES ET AL.: PATHFINDER VENTIFACTS
BRIDGES ET AL.: PATHFINDER VENTIFACTS
BRIDGES ET AL.: PATHFINDER VENTIFACTS

BRIDGES ET AL.: PATHFINDER VENTIFACTS
BRIDGES ET AL.: PATHFINDER VENTIFACTS
BRIDGES ET AL.: PATHFINDER VENTIFACTS
BRIDGES ET AL.: PATHFINDER VENTIFACTS
BRIDGES ET AL.: PATHFINDER VENTIFACTS
BRIDGES ET AL.: PATHFINDER VENTIFACTS
BRIDGES ET AL.: PATHFINDER VENTIFACTS
BRIDGES ET AL.: PATHFINDER VENTIFACTS
BRIDGES ET AL.: PATHFINDER VENTIFACTS
BRIDGES ET AL.: PATHFINDER VENTIFACTS
BRIDGES ET AL.: PATHFINDER VENTIFACTS
BRIDGES ET AL.: PATHFINDER VENTIFACTS
BRIDGES ET AL.: PATHFINDER VENTIFACTS
BRIDGES ET AL.: PATHFINDER VENTIFACTS
BRIDGES ET AL.: PATHFINDER VENTIFACTS
BRIDGES ET AL.: PATHFINDER VENTIFACTS
BRIDGES ET AL.: PATHFINDER VENTIFACTS
BRIDGES ET AL.: PATHFINDER VENTIFACTS
BRIDGES ET AL.: PATHFINDER VENTIFACTS